Applied Catalysis B: Environmental 127 (2012) 371–388

Contents lists available at SciVerse ScienceDirect

Applied Catalysis B: Environmental

journal homepage: www.elsevier.com/locate/apcatb

Review

Low and non-platinum electrocatalysts for PEMFCs: Current status, challenges and prospects

A. Brouzgou [a], S.Q. Song [b,**], P. Tsiakaras [a,*]

[a] Department of Mechanical Engineering, School of Engineering, University of Thessaly, Pedion Areos, 38334 Volos, Greece
[b] State Key Laboratory of Optoelectronic Materials and Technologies/The Key Lab of Low-carbon Chemistry & Energy Conservation of Guangdong Province, School of Physics and Engineering, Sun Yat-sen University, Guangzhou 510275, China

ARTICLE INFO

Article history:
Received 3 May 2012
Received in revised form 2 August 2012
Accepted 28 August 2012
Available online 5 September 2012

Keywords:
Low Pt loading electrocatalysts
Non-Pt electrocatalysts
H_2-PEMFCs
DMFCs
DEFCs

ABSTRACT

Platinum-based nanomaterials are the most commonly adopted electrocatalysts for both anode and cathode reactions in *polymer electrolyte membrane fuel cells* (PEMFCs) fed with hydrogen or low molecular alcohols. However, the scarce world reserves of Pt and its high price increases the total cost of the system and thus limits the feasibility of PEMFCs. Based on this problem, for PEMFCs to have wide practical applications and become commercially viable, the challenging issue of the high catalyst cost resulting from the exclusive adoption of Pt or Pt-based catalysts should be addressed. One of the targets of the scientific community is to reduce the Pt loading in *membrane electrode assemblies* (MEAs) to *ca.* 150 $\mu g\ cm^{-2}_{MEA}$, simultaneously maintaining high PEMFCs performances. The present paper aims at providing the state-of-the-art of low Pt and non-Pt electrocatalysts for: (a) *H_2-O_2 PEMFCs*, (b) *Direct Methanol Fuel Cells* (*DMFCs*) and (c) *Direct Ethanol Fuel Cells* (*DEFCs*). The detailed analysis of a big number of recent investigations has shown that the highest mass specific power density (MSPD) value obtained for *H_2-O_2 PEMFCs* has far exceeded the 2015 target (5 mW $\mu g^{-1}_{Pt_{total}}$) set by the USA department of energy, while a several number of investigations reported values between 1 and 5 mW $\mu g_{Pt}{}^{-1}$. However, the highest values measured under DMFCs and DEFCs working conditions are still relatively low and close to 0.15 and 0.05 mW $\mu g_{Pt}{}^{-1}$ respectively. Moreover, the last years, promising results have been reported concerning the design, fabrication, characterization, and testing of novel non-Pt (Pt-free) anodes and cathodes for PEMFCs applications.

Contents

* Corresponding author. Tel.: +30 24210 74065; fax: +30 24210 74050.
** Corresponding author. Tel.: +86 20 84113253; fax: +86 20 84113253.
E-mail addresses: stsssq@mail.sysu.edu.cn (S.Q. Song), tsiak@mie.uth.gr (P. Tsiakaras).

0926-3373/$ – see front matter © 2012 Elsevier B.V. All rights reserved.
http://dx.doi.org/10.1016/j.apcatb.2012.08.031

1. Introduction

It is well known that *polymer electrolyte membrane fuel cell* (PEMFC) *systems* are intended to be used for transportation and portable applications as well as for stationary ones, mainly due to their low temperature operation and quick start-up. In these systems, hydrogen is considered as the preferred fuel in virtue of its high activity and environmental benignity. Fuel cell is considered as one of the most promising products of 21st Century, as it can compete, in terms of efficiency, with batteries, internal combustion engines and power grids. The challenge is whether fuel cell can be made with a reasonable price.

Along with the PEMFCs' development, low molecular weight alcohols, especially methanol and ethanol which have also been examined as alternative fuels to hydrogen mainly because they are easily handled due to their liquid form and high mass energy density and can be directly fed to the anode without reforming.

Whatever the case may be, Pt or Pt-based binary or ternary catalysts are still the well-known and commonly-adopted materials providing the highest activity for electrode reactions and lifetime stability. Nevertheless, the total Pt reserves in the world will be depleted if each vehicle, which is powered by a 75 kW fuel cell stack, needs approximately 75 g of Pt (~1 mg Pt/W) [1]. More precisely, one and a half billion cars will require more than 110,000 tons of Pt, which is far more than the world-wide estimated Pt reserves (~28,000 tons) [2], in addition to the other applications of Pt in the area of catalysis, jewellery and so on. To the above reasons, it should also be added the high cost of Pt (Fig. 1) [3], which is one of the main obstacles to PEMFC's commercialization.

Therefore, in order to increase Pt's utilization coefficient and consequently decrease its content, the research and development has shot either to Pt-based electrocatalysts with low-Pt loading, which are usually dispersed on carbon supports with high specific surface area [4], or to non-Pt (Pt-free) electrocatalysts. Moreover, the cost target of ~30 $/kW (current Internal Combustion Engine's cost) that has been set for 2015 and can be met only if the maximum mass specific power density (max-MSPD) will be reduced to less than 200 mg of Pt_{total} per kW (higher than 5 mW $\mu g^{-1}_{Pt_{total}}$) at cell voltages higher than 0.65 V (U.S. Department of Energy, DOE). This cost reduction could be achieved: (a) by increasing the power density to 0.8 – 0.9 W cm^{-2}_{MEA} at cell voltages >0.65 V, (b) by reducing mass transfer loss at higher current densities, and (c) by reducing Pt-loading in MEAs to < 150 $\mu g\,cm^{-2}_{MEA}$ (Fig. 2) [5]. The present work aims at providing the state-of-the-art of low-Pt and non-Pt (Pt-free) electrocatalysts (anodes and cathodes) developed for: (a) H_2-O_2 PEMFCs, (b) Direct Methanol Fuel Cells (DMFCs) and (c) Direct Ethanol Fuel Cells (DEFCs).

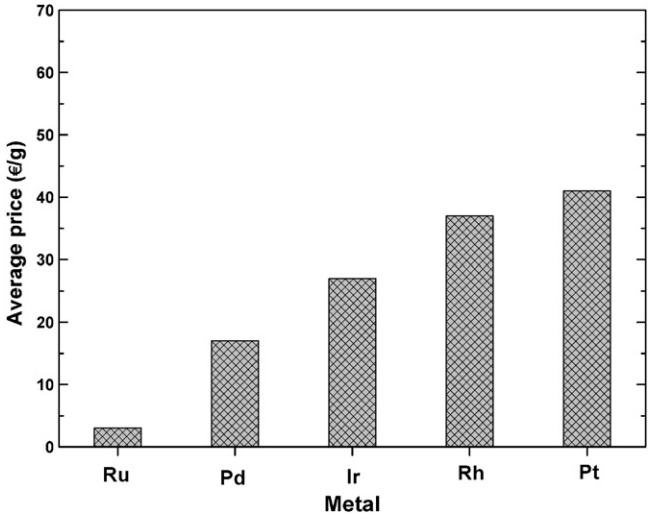

Fig. 1. The average price in Euro per gram of noble metal last year [3].

2. Low platinum electrocatalysts

2.1. Anodes

Platinum has been considered as the best catalyst for the electrochemical reactions that take place in the anode compartment of PEMFCs, but accounts for about 50% of the fuel cells cost [5]. To accelerate breakthroughs in PEMFCs' R&D and their sustainable commercialization, great effort has been devoted by a number of research groups world-wide in order to decrease the Pt loading at a level of lower than 150 $\mu g\,cm^{-2}_{MEA}$ [5] (or <200 $mg_{Pt}\,kW^{-1}$ or <15 g_{pt} for a 75 kW vehicle) (DOE). In this section, it is reported and discussed the research and development of the last decade devoted to low-platinum PEMFCs' anode electrocatalysts for: (a) Hydrogen Electro-oxidation Reaction (HOR), (b) Methanol Electro-oxidation Reaction (MOR), and (c) Ethanol Electro-oxidation Reaction (EOR).

2.1.1. H_2-PEMFCs

The adsorption of H_2 on metal electrodes such as Pt has been extensively studied in H_2-PEMFCs. As far as the HOR is concerned, it is well known that due to its quite facile kinetics on Pt, its corresponding overpotential can be negligible even at high current

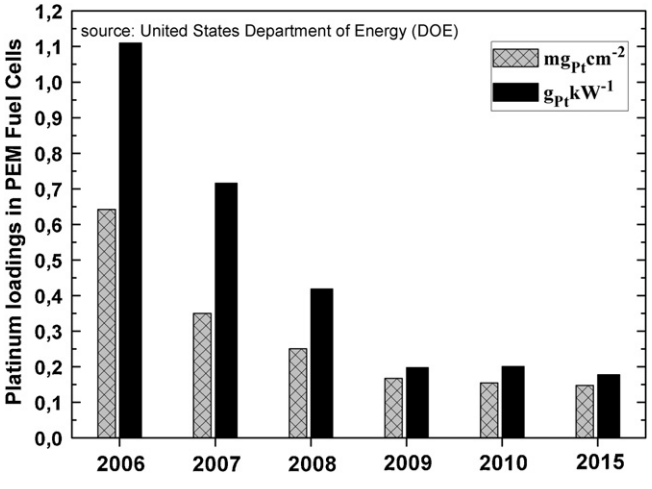

Fig. 2. Platinum loading target in terms of mg cm^{-2} and g kW^{-1} for H_2-O_2 PEMFCs: 2006–2015 [2].

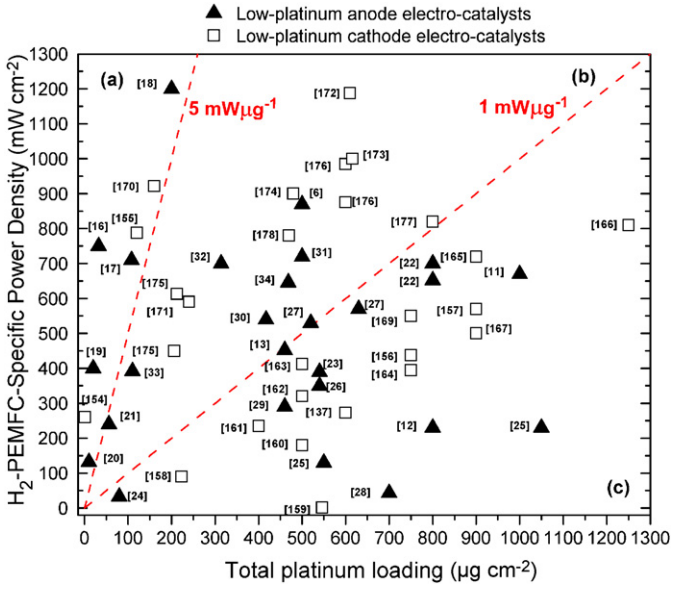

Fig. 3. H_2-PEMFC operation results: Maximum Power Density (mW cm^{-2}) dependency on total (anode + cathode) Pt loading ($\mu g\,cm^{-2}$). In the brackets the reference number is reported.

density values. Thus, most H_2-PEMFCs adopted Pt as HOR anode material, but as it is aforementioned Pt reserves are not enough and its price is very high. Today, in order to reduce the cost of H_2-PEMFCs, platinum alloys are considered as a plausible solution. The combination of Pt with another metal can improve the electrocatalytic activity. For example, the replacement of Pt/C by PtPd/C with a 1:1 Pt:Pd atomic ratio, leads to a 35 wt. % of Pt reduction [6]. Following this direction, many alloys were studied using mainly Ru as the second metal and a third component such as W [7], Sn [7], Os, Pd [8], Co, Ir, Mn, Cr [9], Au, Ag, Rh, or W_2C [10] to form binary and ternary alloys respectively. It was found that the binary alloys, due to the efficient synergetic action between Pt and Ru, or to the electronic effect of Ru on Pt, exhibited enhanced catalytic activity even in presence of CO [11,12]. Another effective way to decrease Pt loading is the adoption of high specific surface area supports to enhance both Pt dispersion and utilization coefficient. To this purpose, novel carbon materials with special nano-scale surface structures have been developed, offering some advantages compared to the commonly and widely adopted XC-72R carbon black (Cabot Corp.) such as: higher surface area, higher conductivity, higher stability etc. [13,14]. As a result, through the above attempts the total Pt loading (anode + cathode) in H_2-PEMFCs the last decade has been dramatically reduced [15] and there is still room for further reduction. As it has been expressed by the DOE of the USA, the target for H_2-PEMCs until 2015 is 200 $mg_{Pt_{total}}\,kW^{-1}$ or 5 mW $\mu g^{-1}_{Pt_{total}}$. In this section, the low-Pt anode catalysts are discussed. More precisely, Fig. 3 summarizes the results of the main investigations, appeared the last decade in the international literature, concerning both low-Pt anode and low-Pt cathode catalysts for H_2-PEMFCs. As it can be clearly seen, the results could be classified into three main regions of maximum mass specific power density (max-MSPD) values: (a) higher than 5 mW $\mu g^{-1}_{Pt_{total}}$, (b) between 1 – 5 mW $\mu g^{-1}_{Pt_{total}}$ and (c) lower than 1 mW $\mu g^{-1}_{Pt_{total}}$. In region (a), there are few catalysts which meet the MSPD target of > 5 mW $\mu g^{-1}_{Pt_{total}}$. More precisely, the reported maximum MSPD, 23.5 mW $\mu g^{-1}_{Pt_{total}}$ (750 mW cm^{-2}; 32 $\mu g_{Pt}\,cm^{-2}$), has been achieved by Sung et al. [16]. A carbon supported Pd-based PdPt catalyst with an atomic ratio 19:1 has been fabricated by the conventional sodium borohydride reduction method combined with freeze-drying. As cathode a Pt/C electrocatalyst has been used. The amount of the platinum was only 5 at. % Pt (19:1 atomic ratio of Pd:Pt) showing that Pd-based catalysts can successfully enhance the PEMFCs' performance. Antolini et al. [17] also examined Pd-based catalysts. According to their results the MSPD was 6.57 mW $\mu g^{-1}_{Pt_{total}}$ (710 mW cm^{-2}). The electrocatalysts were prepared by the reduction of metal precursors with formic acid, managing a total platinum loading of 108 $\mu g_{Pt}\,cm^{-1}$ (96:4 atomic ratio of Pd:Pt).

Manthiram et al. [18], fabricated a high performance MEA (1200 mW cm^{-2}, 200 $\mu g_{Pt}\,cm^{-2}$) by a modified thin-film method using un-catalyzed gas diffusion electrodes to support the thin film catalysts layer. The anode and the cathode catalysts were Pt supported on carbon black with a loading of 100 $\mu g\,cm^{-2}$ for each electrode. As it is observed, despite the very low Pt loading, this electrocatalyst presented the highest power density values. Cavarroc et al. [19] manufactured ultra-low Pt content MEA (10 $\mu g\,cm^{-2}$ for the anode and 10 $\mu g\,cm^{-2}$ for the cathode) by magnetron co-sputtering of carbon and Pt on a uncatalyzed gas diffusion layer, which gave a power density of 400 mW cm^{-2} or 20 mW $\mu g^{-1}_{Pt_{total}}$. Additionally, Gruber et al. [20] also sputter-deposited Pt thin film layers onto different porous electrodes, as the platinum thin film layer presents the advantage to be active in the immediate neighbourhood of the electrode with the proton-conducting membrane. The total Pt loading was only 10 $\mu g\,cm^{-2}$ and the maximum *mass specific power density* almost reached 13.2 mW $\mu g^{-1}_{Pt_{total}}$ (132 mW cm^{-2}) (Fig. 3, region a). The aforementioned works managed to decrease the Pt amount and simultaneously increase its utilization coefficient. To reduce Pt loading, except for the trend to alloy the Pt or to modify its support, a proper MEAs fabrication method could also be a promising way. Erlebacher et al. [21] suceeded to control very low values of Pt loading (56 $\mu g\,cm^{-2}$ of total platinum loading) by adopting a stamping technique and then to fabricate Pt-plated nanoporous gold leaf, which is a carbon-free electrocatalyst. Despite of the very low Pt amount, they obtained 4.28 mW $\mu g^{-1}_{Pt_{total}}$ (240 mW cm^{-2}).

As it can be distiguished in Fig. 3, a serious number of investigations have also been appeared [11,12,22–29] the last decade with fuel cell *maximum mass specific power density* values below 1 mW $\mu g^{-1}_{Pt_{total}}$ (region c, in Fig. 3), while for some others [6,13,30–34] the values are embraced in the range between 1 – 5 mW $\mu g^{-1}_{Pt_{total}}$ (region b, Fig. 3). From a quick glance at the catalysts that belong to regions (b) and (c), it is deduced that in the last years one of the common approaches to succeed the Pt loading target was to adopt also novel supports, except carbon black. Among the most examined supports, are the *multi-walled carbon nanotubes* (MWCNTs) and *single-walled carbon nanotubes* (SWCNTs), which possess desirable properties as the Pt supports, such as high electrical and thermal conductivity, inertness, etc. [35].

2.1.2. Direct methanol fuel cells – DMFCs

DMFCs mainly have the following technical drawbacks: (i) low electrocatalytic activity for *methanol oxidation reaction* (MOR), (ii) very low electrocatalytic activity for *oxygen reduction reaction* (ORR) especially in presence of methanol crossover, and (iii) CO poisoning of the anode electrocatalyst. From one hand, the sluggish MOR kinetics even over PtRu, which is one of the best catalytic systems developed for this reaction, is one of the determining steps for DMFCs commercialization. On the other hand, the best catalytic systems exhibiting a desirable DMFCs performance require a quite high anode catalyst loading of 200 – 800 $\mu g\,cm^{-2}$ [36]. Thereafter, in the identification of novel anode catalysts for MOR, not only the performance (activity, reliability, and durability) but also the cost should be taken into account. Consequently, even in this case, one effective strategy for low cost anode catalysts development is to

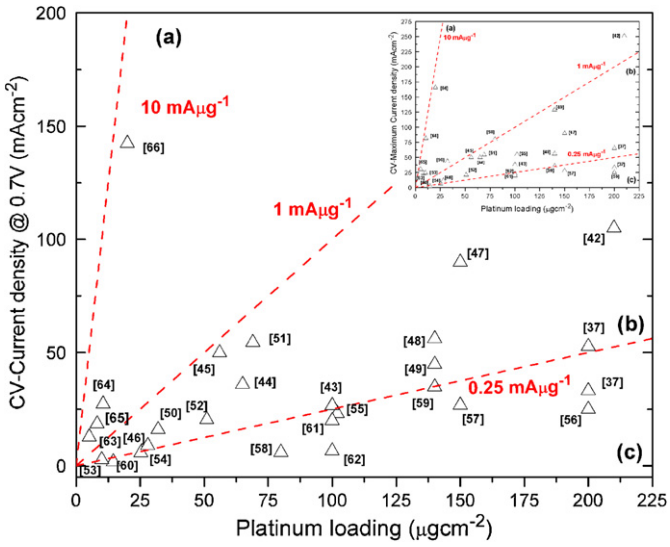

Fig. 4. Cyclic voltammetric results for MOR: Current density ($mA\,cm^{-2}$ at 0.7 V) dependency on the platinum loading ($\mu g\,cm^{-2}$) for methanol electro-oxidation. Inset: Maximum current density dependency on the platinum loading ($\mu g\,cm^{-2}$) for methanol electro-oxidation. In the brackets the reference number is reported.

reasonably decrease the Pt content, while maintaining the DMFCs performance at an accepted level.

According to the literature, a number of Pt alloys [37,38], with Pt-Ru [36] to be the best, exhibited an enhanced electrocatalytic activity for MOR by removing CO-like intermediates through bifunctional mechanism at lower potential values. The catalytic activity of Pt-Ru-alloys [37] towards MOR, compared to the other Pt alloys, has been extensively studied by different research groups. Among them, Whitacre et al. [39] investigated a low Pt loaded catalyst ($Ni_{31}Zr_{13}Pt_{33}Ru_{23}$) with comparable specific activity towards MOR to the best Pt-Ru alloy. Currently, Ando et al. [40] adopted a new synthesis method that involve the following steps: (a) oxidation of carbon support, (b) adsorption of Pb^{2+}, (c) its reduction and (d) galvanic displacement of Pb^0 by Pt and Ru, to finally develop very thin Pt-Ru nanoplatelets on carbon nanoparticles. This catalyst exhibited 10 times higher Pt mass activity towards MOR than the commercial PtRu/C, while its Pt loading was only $0.32\,\mu g_{Pt}\,cm^{-2}$, much less than the commercial one ($10\,\mu g_{Pt}\,cm^{-2}$). This significant activity improvement has been attributed to the effect of the *underlying layer*, which strongly affected the activity of the *top layer* catalyst. Novel mesoporous alloys Pt-Ru ($116\,\mu g_{PtRu}\,cm^{-2}$) were investigated by Corti et al. [41]. Compared to Pt itself, Pt/Ru alloy containing *ca.* 3 at.% of Ru and $\sim 112\,\mu g_{Pt}\,cm^{-2}$, exhibited lower onset potential value and 5% higher than the E-TEK's Pt/C. This behaviour is assigned to the larger pore size of the mesoporous Pt and PtRu catalysts characterized with this template that seems to improve the methanol accessibility to the active sites.

The state-of-the-art of the low Pt loading electrocatalysts activity at 0.7 V and maximum activity for MOR obtained by the cyclic voltammetry technique under half cell conditions is depicted in Fig. 4. The 0.7 V (instead of 0.4 V, which is considered as the working voltage of DMFC in a practical fuel cell) has been selected for the comparison of the catalysts as most of the peak current densities are close to this potential value. The results of the characterized catalysts are classified into three distinct regions of mass specific activity (MSA) values: (a) between $1\,mA\,\mu g_{Pt}^{-1}$ and $10\,mA\,\mu g_{Pt}^{-1}$, (b) between $0.25\,mA\,\mu g_{Pt}^{-1}$ and $1\,mA\,\mu g_{Pt}^{-1}$, and (c) lower than $0.25\,mA\,\mu g_{Pt}^{-1}$. From the above regions, it is evident that most of the examined electrocatalysts [37,42–53] present intermediate electrocatalytic activity (region b, in Fig. 4), while the number of works [37,54–62] which present lower mass specific activity ($< 0.25\,mA\,\mu g_{Pt}^{-1}$, region c) is also not small. Only few works [63–66] belong to region (a). The best value has been obtained by Yang et al. [66]. This research group reported for the first time the synthesis of core-shell CdSe at Pt nanocomposites. The Pt loading was $20\,\mu g_{Pt}\,cm^{-2}$, while the current density at 0.7 V reached $142.5\,mA\,cm^{-2}$ vs. Ag/AgCl ($165\,mA\,cm^{-2}$, maximum current density), which is the highest among the values of the electrocatalysts, appeared in the international literature.

In general, bimetallic nanomaterials with core-shell structure usually exhibit superior activity in heterogeneous catalysis due to the synergetic effect between the two metals, while the metal is distributed only on the surface of a core composed of a transition metal other than Pt. Thus the Pt loading can be decreased. Moreover, most of them showed remarkable CO_{ads} tolerance and more effective mechanism for promoting CO_{ads} removal [63]. According to the literature analysis (Fig. 4), except the special structure, adopting different supports is also an effective way to reduce Pt loading, the same as the case of H_2-PEMFCs. Among the investigated novel carbon materials, the pre-treated CNTs are extremely attractive. The use of nanotechnology for treating catalyst support is very significant as it contributes to a high Pt utilization and an increased specific surface area. More precisely, by improving Pt utilization, its loading is minimized and the performance is improved. In the catalyst layer, this can be accomplished by a better distribution of the platinum particles, or a smaller particle size, or an increase of the number of the particles in the three-phase boundary region [67]. Consequently, the characteristics of the support materials can also determine the electrochemical properties of the catalysts by altering: (i) the active electrochemical surface area, (ii) the metal catalysts stability during the fuel cell operation and (iii) the mass transfer. Hence, the optimization of carbon supports is very important in DMFC technology development [35]. Tang et al. [68] reviewed new carbon materials such as ordered porous carbon, carbon nanofibers, etc., which have been used in direct alcohol fuel cells. According to them, these materials generally presented better performance due to their special structure, better crystallinity, good stability and faster mass transfer compared to the commercial materials, with carbon nanotubes to demonstrate the best performance up to the present [69].

In this point, it is noted that in the inset of Fig. 4 the comparison of the reported catalysts is done taking the maximum current density as reference point instead of the current density at 0.7 V. However, the results are almost the same, except that reported by Rao et al. [42]. They studied the promoting role of the molybdenum oxides in Pt to the methanol oxidation reaction and measured (CV) a current density of $251\,mA\,cm^{-2}$ vs. Ag/AgCl.

Meanwhile, despite the fact that many low Pt loading anode electrocatalysts have been examined for MOR by using the cyclic voltammetry technique (Fig. 4), a relatively small number of catalysts have been investigated under real DMFC operational conditions.

The up-to-date low Pt anode and cathode DMFCs' electrocatalysts and for the sake of comparison some examples of the best reported electrocatalysts with high total Pt loading are depicted in Fig. 5. The results can be classified into three regions: region (a) which embraces the catalysts with maximum *mass specific power density* higher than $0.1\,mW\,\mu g_{Pt_{total}}^{-1}$, region (b) which includes the catalysts with maximum *mass specific power density* between $0.01\,mW\,\mu g_{Pt_{total}}^{-1}$ and $0.1\,mW\,\mu g_{Pt_{total}}^{-1}$, and region (c) with maximum *mass specific power density* lower than $0.01\,mW\,\mu g_{Pt_{total}}^{-1}$. The lowest total Pt loading reported is $730\,\mu g_{Pt_{total}}\,cm^{-2}$ and it has been studied under DMFC conditions (region a, in Fig. 5) by Gonzales et al. [70]. They prepared carbon-supported anode Pt-Sn electrocatalysts, by co-impregnation of Pt and Sn precursors with formic acid as the reducing agent. The examined electrocatalyst

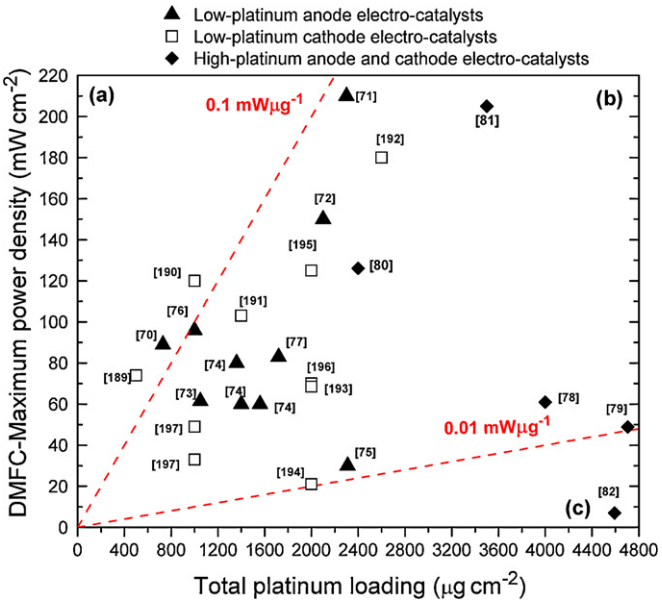

Fig. 5. *Direct Methanol Fuel Cell* operation results: Maximum DMFCs power density dependency on total (anode + cathode) platinum loading ($\mu g\,cm^{-2}$). In the brackets the reference number is reported.

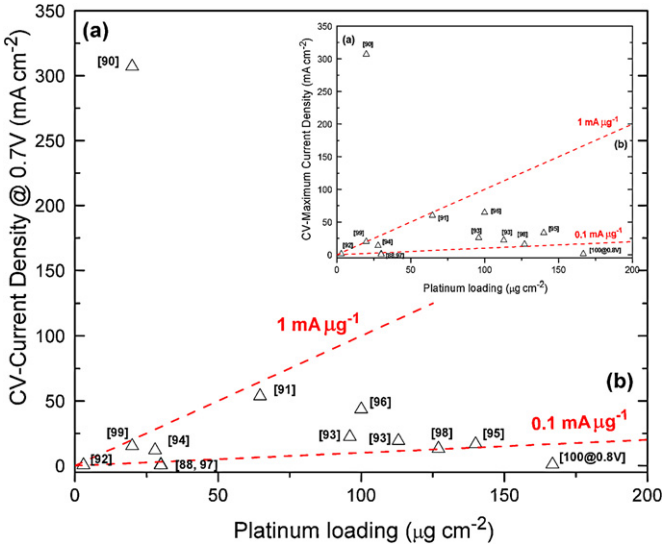

Fig. 6. Cyclic voltammetric results: Current density ($mA\,cm^{-2}$ at 0.7 V) dependency on the platinum loading ($\mu g\,cm^{-2}$) for ethanol electro-oxidation. Inset: Maximum Current Density dependency on the platinum loading ($\mu g\,cm^{-2}$) for ethanol electro-oxidation. In the brackets the reference number is reported.

exhibited performance, $89\,mW\,cm^{-2}$ ($0.12\,mW\,\mu g^{-1}_{Pt_{total}}$). According to the authors [70], Pt-Sn with an appropriate atomic ratio of Pt:Sn oxidizes CO at lower potentials than pure Pt. Therefore, in this work the good DMFC performance could be attributed to the Pt-Sn alloy effect and its synergistic action on CO removal.

According to the state of the art, the highest fuel cell performance ($210\,mW\,cm^{-2}$ or $0.09\,mW\,\mu g^{-1}_{Pt_{total}}$) was achieved over a PtRu alloy supported on graphitic mesoporous carbon [71] and it has been attributed to the crucial role of the mesoporous carbon pore size.

The second best fuel cell performance of $150\,mW\,cm^{-2}$ or $0.07\,mW\,\mu g^{-1}_{Pt_{total}}$ has been reported by Aricò et al. [72], over Pt-decorated ($2100\,\mu g_{Pt_{total}}\,cm^{-2}$) unsupported Ru electrocatalyst. Most of the reported results in Fig. 5 have been obtained at anodes with total Pt loading higher than $1000\,\mu g_{Pt_{total}}\,cm^{-2}$ (region b) [71–81]. Region (c) contains the results of high Pt loading anode with very low performance [82].

It is a fact that year by year the anode Pt loading is significantly reduced along with the improvement of catalyst synthesis methods, MEA fabrication techniques, and so on. Nevertheless, despite of the attempts and the improvements to lower Pt loading in order to achieve a desirable DMFC performance, the total Pt loading (anode + cathode) still remains very high. More precisely, as it has been mentioned above, today the acceptable mass specific power density (MSPD) target for H_2-PEMFCs is $\sim 5\,mW\,\mu g^{-1}_{Pt_{total}}$. If the same or at least the half target will be adopted from the international research community for DMFCs, it is obvious that much stronger effort is necessary for their commercialization. This is due to the fact that up to now the best DMFC mass specific power density value is close to $0.12\,mW\,\mu g^{-1}_{Pt_{total}}$ [70] (Fig. 5).

2.1.3. Direct ethanol fuel cells—DEFCs

Aricò et al. [83] was one of the first research groups that investigated the electrochemical oxidation of ethanol in a liquid-feed solid polymer electrolyte fuel cell operating at 145 °C. The products were water, carbon dioxide, acetaldehyde and unreacted ethanol. Based on the state-of-the-art of anode electrocatalysts for *Ethanol Oxidation Reaction* (EOR) in DEFCs, the main products of this reaction are still acetaldehyde, acetic acid [84], and CO_2 [85] in relatively low quantities. Consequently, identifying electrocatalysts for oxidizing ethanol to CO_2 that can break C-C bonds of ethanol molecules has become a practical challenge for DEFCs' development. In addition, the imperative necessity for lowering Pt loading by doping Pt with a second or a third metal has been seriously taken into account. According to Antolini's review up-to 2007 about EOR electrocatalysts [86], the anode materials that have been extensively investigated were the binary Pt-Ru and Pt-Sn and the correlated ternary Pt-Ru and Pt-Sn based catalysts, with an average Pt loading of $2000\,\mu g_{Pt}\,cm^{-2}$. Based on the current status of EOR anode electrocatalysts, the above-mentioned metal combinations are still the preferable ones. For example, it has been reported that the addition of two metals such as RuSn and RhSn enhances the electrocatalytic activity toward EOR with respect to Pt alone or binary PtSn or PtRu. More precisely, at lower potentials Sn exhibits higher activity than Pt to activate water molecules forming OH species that can further react with the adsorbed acetaldehyde molecules to produce acetic acid [87]. In Fig. 6, the current density from CV as a function of platinum loading are plotted and two main regions can be distinguished: region (a) which embraces electrocatalysts with mass specific activity higher than $1\,mA\,\mu g^{-1}$, and region (b) where the mass specific activity is between $0.1 - 1\,mA\,\mu g^{-1}_{Pt}$.

Recently, Adzic's group [88] reported a ternary $PtRhSnO_2$ electrocatalyst consisted of $\sim 30\,\mu g_{Pt}\,cm^{-2}$ (30 nmol of Pt) and $4.1\,\mu g_{Ru}\,cm^{-2}$ (8 nmol of Rh). Despite the fact that Rh loading was very low, its presence dramatically enhanced the C-C bond cleavage of ethanol molecules, in acidic environment even at room temperature, mostly due to the joint synergetic effect among the components. Although Rh additive can improve PtSn's activity, the composite catalyst is still a relatively Pt-rich high cost material not to mention that the price of Rh is almost the same with that of Pt ($\sim 45€/g_{Pt}$ vs. $\sim 40€/g_{Rh}$). The role of Ru-oxide in the Pt-Ru alloy catalysts has been lately recognized by Datta et al. [89]. They found that under the optimum composition ($Pt_{88}Ru_{12}$) the onset potential was very low and the current density for EOR reached the value of $40\,mA\,cm^{-2}$ vs. MMS under linear sweep voltammetry (LSV) measurements.

As it can be seen in Fig. 6 only one result is contained in region (a), recently reported by Wang et al. [90]. They prepared and tested a carbon-supported PtRuCo nanoparticles with low noble metal content (Pt loading of $20\,\mu g_{Pt_{total}}\,cm^{-2}$), which exhibited

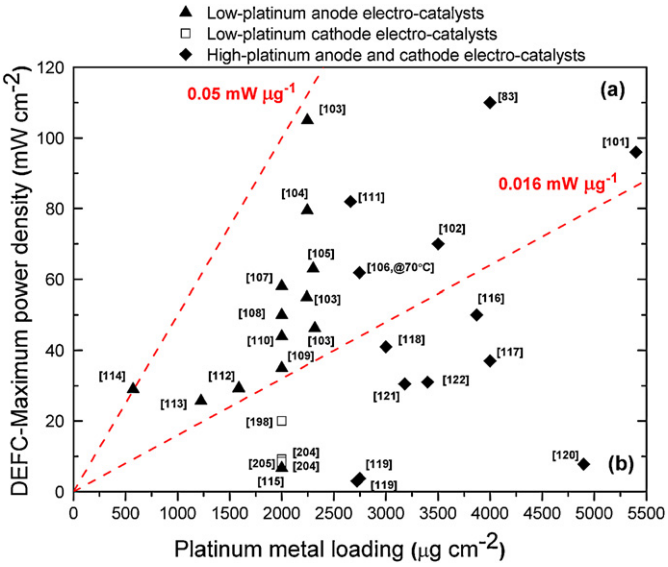

Fig. 7. *Direct Ethanol Fuel Cell* operation results: Maximum DEFCs power density dependency on total (anode + cathode) platinum loading ($\mu g\,cm^{-2}$). In the brackets the reference number is reported.

superior performance of ~307 $mA\,cm^{-2}$ towards EOR. According to the authors, the good performance and stability of the above electrocatalyst could be attributed to the coexistence of Ru and Co. Ru can transform CO-like poisoning species on Pt into CO_2, leaving free the Pt active sites for further adsorption and oxidation of ethanol molecules by the bifunctional mechanism and/or a ligand effect, while Co can improve the EOR performance in acidic solution. Moreover, as it can also be distinguished in Fig. 6 most of the examined catalysts belong to region (b), presenting mass specific activity values between 0.1 – 1 $mA\,\mu g_{Pt}^{-1}$, and higher stability than pure Pt/C [91–100]. A relatively good mass specific activity of *ca.* 0.9 $mA\,\mu g_{Pt}^{-1}$ has been measured over PtRu electrocatalysts. These electrocatalysts have been derived from polyoxyethylene bis(amine) functionalized multi-walled carbon nanotubes (POB-MWCNTs) that have been fabricated by electrostatic self-assembly technology, where Pt and Ru precursors were first uniformly distributed on the POB-MWCNTs surface [91]. Among them, special interest is devoted to the heat-treated PtSn at Rh/C [98] which was synthesized by a two-step sequence method. The above catalyst except for the good ethanol electrooxidation showed an enhanced activity also toward acetic acid electrooxidation, which is ethanol's electrooxidation intermediate. Finally, in the inset of Fig. 6 the results in terms of the maximum current density are reported. It can be easily deduced that among the examined electrocatalysts the order of the current density values did not change.

The performance of low platinum anode or cathode catalysts for DEFCs (at ~90°), in terms of maximum power density dependency on total platinum loading (MEA's platinum loading) is reported in Fig. 7. For comparison reasons, the performance of some anode and cathode catalysts with higher platinum loadings is also included. As it can be seen, the results can be distiguished in two main regions: (a) with the catalysts' presented activity between 0.05 $mW\,\mu g_{Pt_{total}}^{-1}$ and 0.016 $mW\,\mu g_{Pt_{total}}^{-1}$ [83,101–114], and (b) with the catalysts' presented activity below 0.016 $mW\,\mu g_{Pt_{total}}^{-1}$ [115–122]. As it is shown, until today the lowest total Pt loading used for DEFCs is 573 $\mu g\,cm^{-2}$, in the case of PtRuIrSn/C catalyst [114], which exhibited a good maximum power density of 29 $mW\,cm^{-2}$, (0.05 $mW\,\mu g_{Pt_{total}}^{-1}$) and long-term stability. The second best *maximum mass specific power density* value (0.047 $mW\,\mu g_{Pt_{total}}^{-1}$, or 105 $mW\,cm^{-2}$) was achieved by Sun et al. [103] using PtRu/C as anode and Pt/C as cathode. However, the ever highest power density (110 $mW\,cm^{-2}$ or 0.028 $mW\,\mu g_{Pt_{total}}^{-1}$) was achieved in 1998 by Aricò et al. [83], at an operating temperature of 145 °C. The anode was Pt-Ru (2 $mg_{Pt}\,cm^{-2}$) binary electrocatalyst and the cathode was Pt (2 $mg\,cm^{-2}$), both supported on carbon. A high performance, 96 $mW\,cm^{-2}$ or 0.017 $mW\,\mu g_{Pt_{total}}^{-1}$, has been also obtained by Sun et al. [101], over double-layer anode and cathode which both consisted of one layer made by Pt_3Sn and a second-layer by PtRu. The best fuel cell performance was observed in the case the Pt_3Sn was the first layer (close to the anode diffusion layer) and the PtRu as the second one (adjacent to the Nafion membrane).

It is worth to be noticed that as in the case of DMFCs concerning the last five years investigations, the nanomaterials [123,124] have attracted great interest because of their unusual catalytic, mechanical, electrical and optical properties. Recently, different kinds of carbon nanomaterials such as hollow graphitic nanoparticles [68], carbon nanotubes [48] and graphitic carbon nanofibers [68] were investigated and different fabrication methods have been adopted. These carbon materials can exhibit superior performance compared to the conventional carbon supports for EOR anode catalysts. In conclusion, compared to DMFCs, the best performance of DEFCs, in terms of max-MSPD, is three times lower (see Figs. 5 and 7).

2.2. Cathodes

Compared to *hydrogen oxidation reaction* (HOR), *oxygen reduction reaction* (ORR) is characterized by much more sluggish kinetics, with exchange current density values between 10^{-7} and 10^{-9} $A\,cm^{-2}$, versus 10^{-3} $A\,cm^{-2}$ of the HOR [125,126]. Obviously, the electrocatalysts of ORR play a key role in determining the PEMFCs performance. Until now, Pt is considered as the best ORR electrocatalyst. ORR over Pt takes place mainly through a 4-electron process mechanism. Under typical conditions, the oxygen reduction intermediate species share the electrode's surface with platinum oxide and/or hydroxide compounds as well as with other adsorbed species. The formation of platinum oxide and/or hydroxide compounds shows an irreversible behaviour and so the performance of a Pt electrode may also depend on this. The recent state-of-the-art for low-Pt and Pt-free electrocatalysts for ORR, reviewed by Palacin et al. [127] revealed that the research community adopted many different methods to reduce Pt loading, such as using nanoparticles on various supports, preparing Pt-monolayers supported on suitable metal nanoparticles and 1-D, 2-D and 3-D nanostructures, etc.

The mass activities of the most recent low-Pt ORR electrocatalysts that have been tested according to the rotating disk electrode (RDE) technique are shown in Fig. 8 (at 0.75 V, 1600 rpm) [128–131]. From the RDE theory, the relationship between the kinetic current density and the diffusion-limited current density can be expressed (Paulus et al. [132]) by the following relationship $i_k = (i \times i_d)/(i_d - i)$, where i_d stands for the diffusion-limited current density, i_k for the kinetic current density and i for the current density at each electrode potential, on which the calculated kinetic current densities are based. According to the electrode kinetic theory [133], the kinetic current density can be expressed as $\eta = \alpha - (2.3RT/anF)\log(i_k)$, where η is the overpotential, α is a constant, i_k the exchange current density, R the gas constant, T the temperature, a the electron transfer coefficient, n the electron transfer number in the determining step of ORR and F the Faraday's constant. Then the mass activity values can be calculated from the following equation: $i_m = i_k/\text{metal(Pt)}_{loading}$.

Among the reported electrocatalysts, the dealloyed Pt-Cu (3:1) nanoparticles supported on carbon and annealed at 800 °C for 7 h, prepared by Oezaslan et al. [131] presented the highest mass

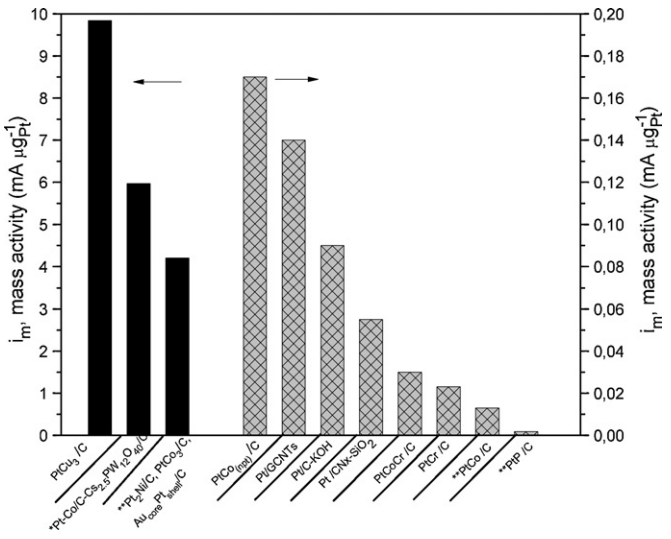

Fig. 8. Mass activities (mA μg_{Pt}^{-1}) (at 0.75 V, 1600 rpm) for *Oxygen Reduction Reaction* (in absence of H_2, MeOH or EtOH), [*1200 rpm, **2000 rpm].

activity, almost 10 mA μg_{Pt}^{-1} vs RHE. The catalyst presented enhanced mass activity, revealing a 4-electron reduction pathway, most probably due to the annealing effect. A new composite electrode was prepared by Dsoke et al. [130]. More precisely, a Pt-Co/C alloy was mixed with a $Cs_{2.5}H_{0.5}PW_{12}O_{40}$ salt, which has been demonstrated to be very effective support for Pt nanoparticles. The as-prepared catalyst exhibited a mass activity of 6 mA μg_{Pt} vs. RHE because of both the high surface activity and the high mobility of the protons. Moreover, the electrocatalysts Pt_2Ni/C [128], $PtCo_3$ [131] and $Au_{core}Pt_{shell}/C$ [129] exhibited similar mass activity values (4 mA μg_{Pt}). The good catalytic activity presented by the Pt_2Ni/C was attributed: (i) to the appropriate interatomic Pt-Pt distance caused by alloying, (ii) to the high dispersion of the alloy catalysts and (iii) to their disordered structure. Concerning the $Au_{core}Pt_{shell}/C$, when Au atoms are exposed to the surface to some extent, the surface Au could repel the adsorption of oxygenated species and higher ORR activity can be achieved. Finally, the annealing at 800 °C for 7 h and the resulting uniformity of Pt–Co crystal phase was the key factor for $PtCo_3$'s good electrocatalytic activity. The mass activity values for the rest of the examined electrocatalysts (Fig. 8) ranged between 0.02 and 0.18 mA μg_{Pt} [134–140].

As it will be also discussed below, despite the fact that many low Pt electrocatalysts, evaluated by the technique of RDE, showed a sufficient activity, it is quite difficult to reduce the cathode's Pt loading without a serious fuel cell performance loss [141,142].

2.2.1. H_2-PEMFCs

A few low-Pt cathode catalysts have been investigated under real H_2-PEMFCs working conditions. Among them, only a small number exceeds the target of 5 mW $\mu g_{Pt_{total}}^{-1}$ which has been set by the USA's DOE (Fig. 3).

The catalytic activity of Pt towards ORR strongly depends on: (i) its O_2 adsorption energy, (ii) the O-O bond dissociation energy, and (iii) the OH binding energy on Pt surface. Alloying causes a lattice contraction, leading to a more favourable Pt-Pt distance for the dissociative adsorption of O_2. The *d*-band vacancy can be increased after alloying, producing a strong metal-O_2 interaction and then weakening the O-O bond.

Binary alloys of Pt-Cu [143], Pt-Co [144–147], Pt-Ni [145,146], Pt-Cr [145] exhibited 2–3 times higher mass specific activity than Pt/C. The enhancement was much greater on the basis of the electrochemical active surface area of Pt. Currently, novel ternary low Pt electrocatalysts, such as PtFeNi and PtFeCo [147] with enhanced electrocatalytic activity towards ORR in PEMFCs have also been reported. However, in some occasions, Pt phase segregation was observed. Because of the lower cost of Pd than that of Pt, Pd-Pt bimetallic catalysts have been extensively examined for ORR, having almost the same electrocatalytic activity as Pt. More precisely, it has been reported that Pd-Pt bimetallic catalysts doped into hollow core mesoporous shell carbon (PtPd/HCMSC) exhibited considerable activity and stability [148,149]. Metal oxide electrocatalysts have also been extensively studied for their ORR catalytic activity and electrochemical behaviour. The investigations showed that in most cases they gave higher ORR performance than Pt/C catalyst. This could be due to their oxygen storage capacity and their ability to exchange oxygen rapidly in the buffer as well as because of their higher durability and good stability with respect to the commercial Pt/C catalysts [150]. Furthermore, core-shell catalysts have recently attracted much attention as part of the efforts to reduce Pt-content. These catalysts have the unique characteristics to force Pt atoms to the surface of the particles containing less expensive metals. Based on the recent investigations, Pt-rich shell and Pt-Co core with low Pt content showed a very good activity. This has been attributed to both the higher surface area, which was caused from the particle surface's leaching Co atoms, and the electronic interaction between Co and Pt atoms [151]. However, as it has been reported by Maillard et al. [152], this dissolution of Co atoms under fuel cell working conditions does not ensure stability of a H_2-PEMFC. The anode was pure Pt supported on carbon. The fuel cell had been operated at 70 °C for 1124 h. A further investigation of the same research group [153] confirmed that Co atoms were continuously depleted from the mother Pt_3Co/C electrocatalyst because they could diffuse from the bulk to the surface of the material. Other methods for reducing Pt loading includes the adoption of novel nano-supports and preparation methods.

Fig. 3 reports the results of the most recent investigations concerning low Pt cathode electrocatalysts tested in a H_2-PEMFC. An optimized electrode structure has been obtained by Mougenot et al. [154] with a Pt loading of 1 $\mu g_{Pt_{total}}$ cm^{-2}. A H_2-PEMFC, with a cathode of PdPt and an anode made by pure Pd, both deposited on different backing layers by the plasma sputtering technique, exhibited a performance of 260 mW $\mu g_{Pt_{total}}^{-1}$, which is the highest MSPD reported in the literature. This result indicates the importance of not only the alloying effect but also the MEAs' fabrication method.

Mukerjee et al. [155] also reported interesting H_2-PEMFC's performance values that exceeded the DOE's 2015 target (6.56 mW $\mu g_{Pt_{total}}^{-1}$ or 788 mW cm^{-2}) using a MEA with 120 μg_{Pt} cm^{-2} of total platinum loading. Their MEA consisted of Pt alone and the electrodes were obtained by direct metallization of non-catalyzed gas diffusion layers via dual ion beam assisted deposition (IBAN) method. This performance was much higher than that of the other electrocatalysts with higher Pt loading (region c) [156–169]. Due to this significant improvement, Mukerjee et al. [170] also adopted the same method for the preparation of MEA with Pt alone, as the electrocatalyst, with a total loading of 160 μg_{Pt} cm^{-2} and mass specific power density *ca.* 5.8 mW $\mu g_{Pt_{total}}^{-1}$ (or 922 mW cm^{-2}). As it can also be seen (Fig. 3), a great number of cathode electrocatalysts [171–178] (region b) presented maximum *mass specific power density* values below 5 mW $\mu g_{Pt_{total}}^{-1}$, while the majority of them [156–169] exhibited performance below 1 mW $\mu g_{Pt_{total}}^{-1}$.

In a summary, a great deal of attention has been given not only to Pt alloys but also to the electrocatalyst preparation methods and support identification. Thus, so far, there is an improvement in H_2-PEMFCs electrocatalysts, with some of them to present maximum mass specific power density values higher than 5 mW $\mu g_{Pt_{total}}^{-1}$.

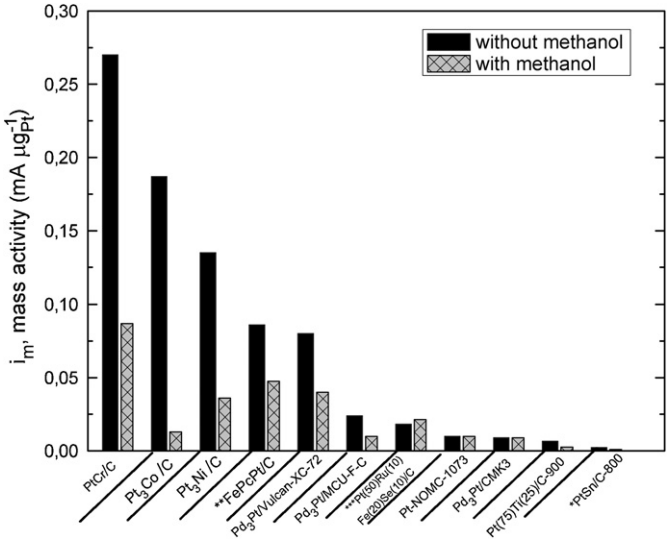

Fig. 9. Mass activities (mA μg_{Pt}^{-1}) (at 0.8 V, 1600 rpm) for *Oxygen Reduction Reaction* in presence and in absence of methanol [*1000 rpm, **1800 rpm, ***2000 rpm].

2.2.2. Direct methanol fuel cells – DMFCs

In the case of DMFCs, the cell performance is normally lower than that of H_2-PEMFCs, while the Pt loading in the catalyst layers is significantly higher, due to the sluggish MOR and ORR at the anode and cathode compartments, respectively. Moreover, in a DMFC, methanol crossover from the anode, through the membrane, to the cathode represents a serious problem which can cause the total fuel cell performance loss. Therefore, methanol-tolerant Pt-based alloys at the cathode are also required for DMFCs. Antolini et al. [179] reviewed methanol-resistant ORR Pt-based electrocatalysts for DMFCs. According to their results, the best performance of the examined electrocatalysts was due to both geometric (decrease of the Pt-Pt bond distance, particle size effect) and electronic (increase of Pt d-electron vacancy) factors [180]. However, at the present there are only few investigations about ORR electrocatalysts for DMFCs with low Pt loading. Fig. 9 depicts the mass activities of some of the most recent low-Pt cathode electrocatalysts in terms of mA μg_{Pt}^{-1} which were examined with the RDE technique for the ORR in presence and in absence of methanol (at 0.8 V, 1600 rpm). According to Fig. 9 the highest mass activity, 0.27 mA μg_{Pt}^{-1} vs. RHE, has been achieved over Pt-Cr alloy nano-sized (50 μg_{Pt} cm^{-2}) supported on carbon (Vulcan XC-72), prepared by Lamy et al. [181] via a Pt-carbonyl route. The relatively good methanol tolerance, exhibited by this catalyst, was attributed to the composition effect and the disordered surface structure. The next better ORR electrocatalyst for DMFCs, Pt_3Co/C, for DMFCs was prepared by Colmenares et al. [182]. Compared to Pt, this catalyst exhibited higher mass activity, at the value of 0.187 mA μg_{Pt}^{-1} vs. RHE (but not very good compared to other catalysts that are depicted in Fig. 9) and a good methanol tolerance, despite its very small particles. The same research group studied also the Pt_3Ni, whose activity reached 0.135 mA μg_{Pt}^{-1} and its tolerance was also good compared to Pt. Wang et al. [183] have studied a new nanocomposite cathode composed of iron phthalocyanine, Pt, carbon black and Nafion (FePc-Pt/C-Nafion), which exhibited enhanced catalytic activity for ORR in absence (0.086 mA μg_{Pt}^{-1} vs. RHE) and in presence of methanol (0.048 mA μg_{Pt}^{-1}) compared with the usual Pt/C based electrodes. However, the rest of the electrocatalysts reported in Fig. 9, even though they present relatively low mass activity values, have excellent tolerance in presence of methanol [184–188].

Generally, there are two different methods reported in the international literature for optimizing methanol tolerant electrocatalysts for ORR: (a) using Pt alloying and (b) using various supports, putting in evidence for the complexity of the synthesis of cheap and efficient electrocatalysts for ORR.

Despite the fact that many low Pt electrocatalysts have been investigated for ORR and characterized by the RDE technique there are only a few ones that have been examined under DMFCs working conditions. In Fig. 5 are depicted the most recent works concerning the investigation of low-Pt ORR electrocatalysts in a DMFC. The published results could be embraced in two regions: region (a) with maximum *mass specific power density* values higher than 0.1 mA μg_{Pt}^{-1} and region (b) with maximum *mass specific power density* values between 0.1 mA μg_{Pt}^{-1} and 0.01 mA μg_{Pt}^{-1}. Similar to the low Pt anodes, the total Pt loading remains relatively high for the low Pt cathodes investigated in a DMFC. According to Fig. 5, the best maximum *mass specific power density* value ~0.15 mW μg^{-1} (or 74 mW cm^{-2}) was achieved by Sakthivel et al. [189]. They prepared Pt electrocatalysts deposited on MWCNTs via the microwave-assisted polyol method (region a), using a zwitterionic surfactant as a stabilizing agent for the formation of Pt nanoparticles. The total Pt loading remained at the relatively low level of 500 μg_{Pt} cm^{-2}. According to the authors, the use of surfactants is another important parameter for the achievement of uniform and stable nanoparticles. Then, the optimized amount, size and distribution of nanoparticles due to the surfactant gave the good maximum *mass specific power density*. Li et al. [190] using Pt-Fe/C (1.2:1) alloy as cathode, with the double amount of Pt 1000 μg_{Pt} cm^{-2}, obtained the second best value ~0.12 mW μg^{-1} (or 120 mW cm^{-2}) reported in the literature. This excellent performance was attributed to the smaller particle size and the better Pt-Fe alloy structure.

However, the majority of the electrocatalysts [191–197] (region b) exhibits maximum *mass specific power density* values between 0.01 and 0.1 mW $\mu g_{Pt_{total}}^{-1}$ (Fig. 5).

2.2.3. Direct ethanol fuel cells – DEFCs

It is well known that in DEFCs, ethanol fed to the anode compartment can permeate through the electrolyte to the cathode, just like methanol in the case of DMFCs. Consequently, ethanol and oxygen adsorption are competing with each other for the same active surface sites. As it was discussed above, DMFCs showed improved performance when Pt-M/C alloys were used as cathode materials instead of Pt/C. In the case of DEFCs, few works [198–200] also showed that the addition of a second metal to Pt enhanced the ORR activity, and that the dependence of the ORR activity on the second metal content reached a maximum [86]. It was found that O_2 is more readily adsorbed and easily dissociated on the M-modified Pt surface. Moreover, in presence of ethanol a larger increase of the ORR overpotential on Pt than on Pt-M has been observed, indicating the higher ethanol tolerance of the binary catalyst [86].

Fig. 10 reports some recent results of low Pt cathode electrocatalysts for the ORR in presence and in absence of ethanol, characterized with RDE technique. As it can be seen, in absence of ethanol the best mass activity of 0.072 mA mg_{Pt}^{-1} is presented by the three Pt-M oxides [201], $Pt_{0.7}$-$Co_{0.3}$/MWCNT [202] and $PtCeO_x$/MWCNT [203]. In presence of ethanol, despite the fact that there were no current peaks associated to the ethanol oxidation, a higher overpotential (in comparison to absence of ethanol) was observed, with $Pt_{0.7}$-$Co_{0.3}$/MWCNT to be more tolerant compared to the other catalysts.

In Fig. 7 are reported the results of the ORR electrocatalysts that have been investigated in a single DEFC. As it can be seen, the number of the investigations devoted to novel ORR electrocatalysts under DEFC operational conditions is very limited, while the hitherto lowest total Pt loading 2000 μg_{Pt} cm^{-2} [198,204,205]. From the small number of the works shown in Fig. 7 it is deduced

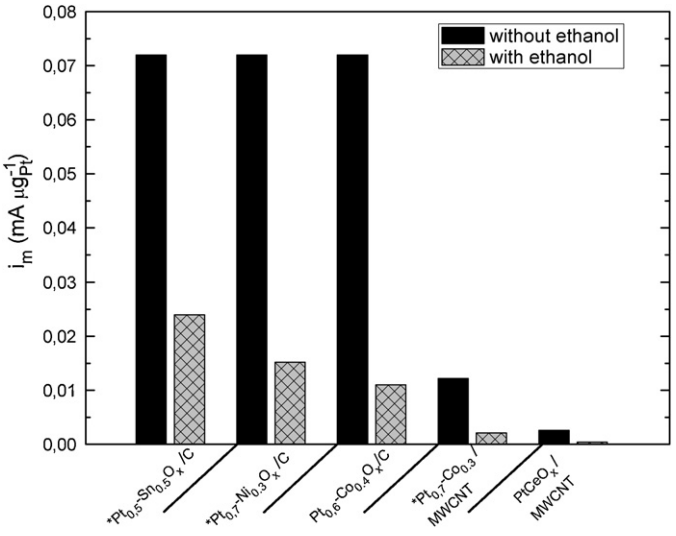

Fig. 10. Mass activities (mA μg_{Pt}^{-1}) (at 0.8 V, 1600 rpm) for *Oxygen Reduction Reaction* in presence and in absence of ethanol [*1200 rpm].

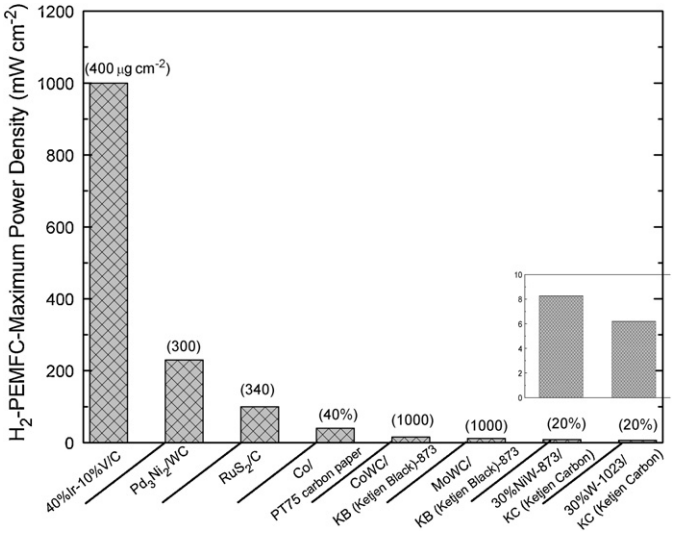

Fig. 11. H_2-Fuel Cell operation results *over non-platinum anodes*: Maximum power density (mW cm^{-2}) over different Pt-free anodes. In the brackets is reported the total platinum amount ($\mu g\ cm^{-2}$) contained in the cathode. Inset: Enlarged bars of the maximum power density of the less active Pt-free electrocatalysts.

that stronger effort is required for further optimization of the DEFC cathodes.

3. Non platinum electrocatalysts

3.1. Anodes

Investigations concerning Pt-free anodes have also appeared recently for H_2-PEMFCs, DMFCs and DEFCs. The corresponding results are presented and discussed below. The challenge of the research community is to develop low cost non-noble metal electrocatalysts, which should have both high electrocatalytic activity and very good stability in a strongly acidic humidified environment of PEMFCs.

3.1.1. H_2-PEMFCs

The last years, a number of scientific works have been devoted to the study of Pd as an alternative electrocatalyst for H_2-PEMFCs [57,206]. Shao et al. [172] reviewed Pd-based electrocatalysts for HOR, but the mechanism of the activity improvement have still not been fully understood. Lee et al. [207] prepared and investigated Pd-Ni alloy supported on tungsten carbide for the HOR. The strong interaction between PdNi alloys and WC in the case of PdNi/WC anode used in a H_2-PEMFC under working conditions caused a performance of 230 mW cm^{-2}, following that of iridium-vanadium alloy which exhibited 1000 mW cm^{-2} (Fig. 11) [208]. The Pt loading of the cathode electrocatalyst was 300 $\mu g\ cm^{-2}$ for the former and 400 $\mu g\ cm^{-2}$ for the latter case. Concerning the PdNi/WC electrocatalyst it is worthy to be noticed that there was no obvious performance degradation after 100 h of continuous operation [208], indicating a long-term stability.

A very common approach to develop non-noble electrocatalysts is to adopt carbides and nitrides [209]. Especially, molybdenum and tungsten carbides and nitrides – cheaper substitutes of Pt-based catalysts – are the most common non-Pt electrocatalysts. The capability of using transition metal carbides and nitrides for HOR has been investigated since the end of sixties by Böhm and Pohl [210]. It has been shown that tungsten carbide/carbon catalyst can be used in fuel cells operated with hydrogen or CO-rich hydrogen fuel. Later, several groups investigated tungsten based materials for HOR [211]. Moreover, it was reported that tungsten carbides showed catalytic properties similar to Pt-group metals [212,213]. From the single fuel cell performance point of view, it was found that in the case of WC and WNi/C the respective maximum power density value obtained was only 5.7 and 7.3% of that achieved over the commercial 20 wt.% Pt/C [212]. Also the maximum power density value over cobalt-tungsten carbide and molybdenum-tungsten carbide with Ketjen carbon support was 14 and 11% of the commercial 20 wt.% Pt/C, respectively [213]. According to the literature, WC containing a small amount of Pt (one-tenth of the amount of Pt contained in the commercial Pt/C catalyst) exhibited superior mass activity and excellent stability to the commercial Pt/C [214] due to the strong synergetic effect between Pt and WC, leading to the drastic reduction of Pt loading. Yang and Wang [215] synthesized and tested in a H_2-PEMFC at 80 °C and 3 atm nano-tungsten carbides electrocatalyst. The electrocatalytic activity at the WC based anode has been attributed to the inherent functionalization of tungsten and carbon valence, as well as to the catalyst nanostructure, which is capable of providing highly active sites.

In order to overcome the Pt loading problem, Kaninski et al. [216] investigated Co (Co/Carbon paper), which costs much less than Pt. Though, the performance of Co towards HOR – not as good as that of Pt – it is higher than that of some other electrocatalysts as it can be seen from Fig. 11.

Usually, non-precious metal alloys are not preferable from the research community, because the requirement of good resistance to CO is difficult to be achieved [217]. As it is obvious from Fig. 11, tungsten carbides and especially nickel carbides are merely suggested for HOR. However, their catalytic activity is not as high as that it was expected compared to the iridium-vanadium alloy investigated by Ma et al. [208]. The fuel cell performance (1000 mW cm^{-2}) was 10 times higher than that obtained over other electrocatalysts with only 400 $\mu g_{Pt}\ cm^{-2}$ at the cathode. The novel Ir-V/C nanoparticles presented not only high activity, but also good stability for more than 100 h fuel cell operation. Moreover, Zhang et al. [218] examined transition metal sulphides (RuS_2/C) for HOR under fuel cell operation and they measured the third better maximum power density value as shown in Fig. 11. The cathode's Pt loading was also relatively low (340 $\mu g_{Pt}\ cm^{-2}$) and the fuel cell performance reached 100 mW cm^{-2}. It is worthy to be noticed that only few investigations concerning non-Pt anodes for HOR have been appeared. However, even in these cases the cathode was loaded with Pt (Fig. 11).

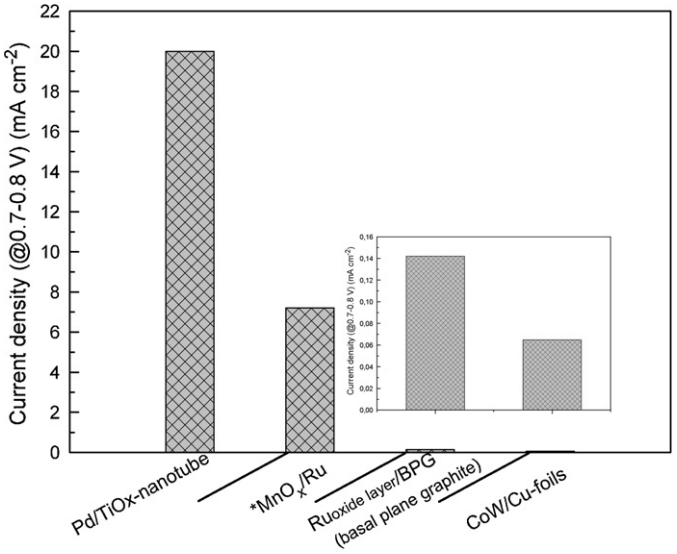

Fig. 12. Cyclic voltammetric results: Current density (mA cm^{-2} at 0.7–0.8 V, and *at 0.15 V) of nonplatinum electrocatalysts for the *Methanol Oxidation Reaction*. Inset: Enlarged bars of the lowest current density values.

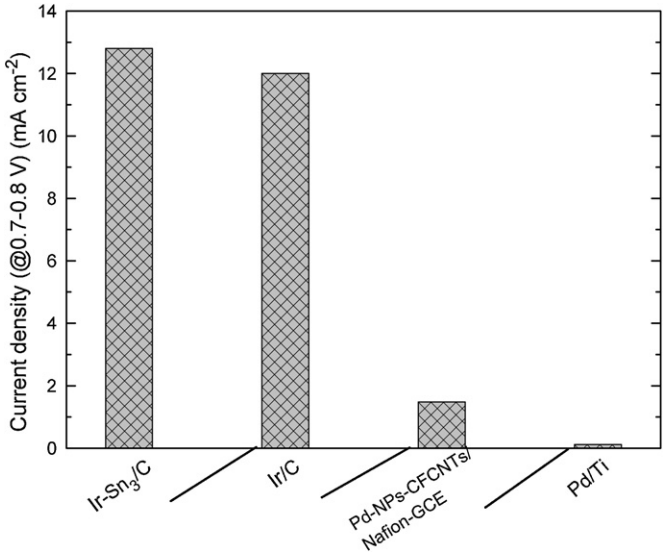

Fig. 13. Cyclic voltammetric results: Current density values (mA cm^{-2} at 0.7–0.8 V) of non-platinum electrocatalysts for the reaction of Ethanol Oxidation.

3.1.2. Direct methanol fuel cells – DMFCs

Few investigations have also been devoted to the development of non-Pt anodes for DMFCs. An interesting review based on transition metal carbides and promoted transition metal oxides as anode catalysts for DMFCs, has been given by Serov et al. [219]. As the authors stated, WC as DMFCs anode in acidic environment presented a good stability. Moreover, they highlighted that transition metal carbides were investigated not only as anode materials, but also as possible supports for Pt electrocatalysts. Recently, some investigations have dealt with tungsten and molybdenum materials as non-Pt anode electrocatalysts for DMFCs. The investigations about the stability of WC and W_2C [220] revealed that WC is stable as anode in acidic environment at 0.6 V, demonstrating the potential application of WC in the electrochemical systems. Novel Co-W alloys supported on Cu-foils for MOR in acidic media has been investigated by Mayanna et al. [221]. As it can be seen in Fig. 12, the Co-W alloy exhibits relatively low activity presenting however good corrosion resistance. According to the authors this behaviour is attributed to the fact that cobalt forms "hard" alloys with tungsten, which are free from surface contamination. Moreover, ruthenium oxide layer supported on basal plane graphite anodes, also exhibited very low catalytic activity [222].

The highest current density (20 mA cm^{-2} vs SCE, Fig. 12) and the second best (7.2 mA cm^{-2} vs. SCE, Fig. 12) towards MOR was achieved over Pd/$TiO_{2nanotubes}$ [223] and MnO_x/Ru [224], respectively. In the first case, Pd/$TiO_{2nanotubes}$ catalyst displayed catalytic activity superior to pure Pd, with the titania to promote the removal of CO. In the second case, the combination of carbon-supported manganese octahedral molecular sieves (OMS-2) with a commercially available Ru-carbon sample showed an enhanced activity.

From the published results, one might conclude that effort has been also devoted in developing non-Pt MOR catalysts. However, from the already published results one might conclude that the complete replacement of Pt affects negatively the electrocatalytic activity towards MOR.

3.1.3. Direct ethanol fuel cells – DEFCs

Pd-based electrocatalysts are the most promising candidates among the non-Pt electrocatalysts. In Fig. 13, two Pd-based electrocatalysts [87,225] are reported, which exhibited lower activity towards EOR compared to iridum-based electrocatalysts. As it can be seen in Fig. 14, the Ir-based EOR electrocatalysts [226] exhibit higher activity than Pt-based electrocatalysts in the activation control region and comparable single DEFC performance with that over Pt_3Sn/C. Consequently, Ir_3Sn/C could be an interesting DEFCs non-Pt anode candidate. However, substantially the problem still remains, because from one side the world reserves of Ir are much lower than that of Pt and from the other the cathode compartment still contains 1000 μg_{Pt} cm^{-2}. As it can be deduced, only few investigations devoted to non-Pt materials for EOR in acidic media have been published, while currently a number of scientific groups try to identify novel electrocatalysts for the EOR in alkaline media.

3.2. Cathodes

Until now, the investigated non-Pt catalysts for ORR, can be mainly classified as follows: (1) porphyrin-based macrocyclic

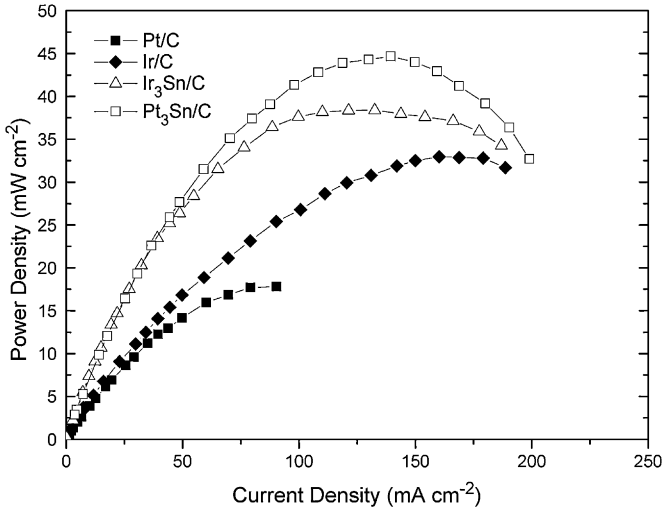

Fig. 14. Polarization curves of a direct ethanol fuel cell employing Ir/C, Ir_3Sn/C, Pt_3Sn/C and Pt/C as anode catalyst respectively. Anode fuel feeding: 1.0 mol L^{-1} ethanol at 1.0 mL min^{-1}, Cell temperature = 90 °C, $P_{cathode}$ = 2.0 bar, anode catalysts with 1.5 mg cm^{-2} of precious metal loading, 1.0 mg cm^{-2} Pt cathode catalyst (40% Pt/C from Johnson Matthey Corp).

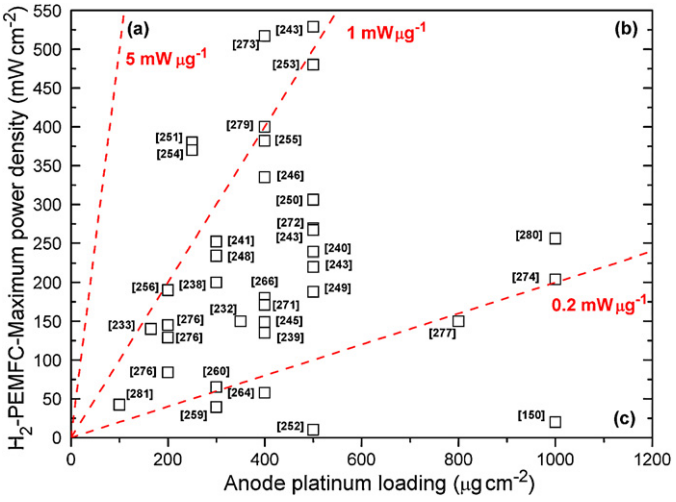

Fig. 15. H_2-PEMFC operation results using non-platinum cathodes and platinum based anodes: Maximum fuel cell power density (mW cm^{-2}) dependency on anode's platinum loading ($\mu g\,cm^{-2}$).

compounds of transition metal (mainly Fe and Co as the central metal) [227], (2) vacuum-deposited Co and Fe compounds [228], (3) metal carbides, nitrides and oxides (FeC_x, MnO_x), (4) Ru-based ($Mo_4R_2Se_8$, Ru_xSe_y, RuN_x)-chalcogenides [229,230]. Moreover, linnaeite Co_xS_y nanocrystals and Co_xSe_y have also lately studied [231]. In Fig. 15 are reported the performances of H_2-PEMFCs that use Pt-free cathode electrocatalysts. Three regions are distinguished: region (a) where the power density values are between 1–5 mW μg_{Pt}^{-1}, region (b) where the power densities values are between 0.2 – 1 mW μg_{Pt}^{-1} and region (c) where the power density values are lower than 0.2 mW μg_{Pt}^{-1}.

3.2.1. H_2-PEMFCs

The examined cathodes for ORR in H_2-PEMFC can be classified as follows:

3.2.1.1. Transition metal macrocycles. One class of non-platinum cathode electrocatalysts that have also attracted attention over the years are the pyrolyzed metal porphyrins, with cobalt and iron porphyrins to be considered as very promising precursors. Among them the most examined ones are CoTMPP/BP (tetramethoxyphenyl porphyrin/black pearls) [232] and CoPPY/MWCNT [233], cobalt-polypyrrole [234], and Fe/Co/TPP [235]. The first two were used as cathode catalysts in a H_2-PEMFC, with performance values of 150 and 140 mW cm^{-2}, respectively (Fig. 15).

3.2.1.2. Nitrogen-based precursors. The transition metal macrocycles, such as porphyrins and phthalocyanines suffer from significant limiting factors, including their cost. Alternative synthesis routes have been explored in order to prepare catalysts with similar active surface species, which were formed during the heat-treatment of transition metal chelates with cheap nitrogen-containing and transition metal containing precursors.

Very recently, Proietti et al. [236] developed Fe-based cathode catalysts exploring the use of a metal-organic-framework as the host for Fe and N precursors; iron(II) acetate and 1,10-phenanthroline, respectively. The as-prepared electrocatalyst has been tested as non-platinum cathode in a H_2-PEMFC performing 910 mW cm^{-2}, which is the highest reported in the literature. The second high non-platinum H_2-PEMFC performance, 430 mW cm^{-2}, was achieved by the same research group [237]. In both cases iron-based catalysts were pyrolysed under the same temperature, 1050 °C, for different time. Except for the high power density, the examined catalysts presented also a good stability when fuel cell's cathode was fed with air. A new non-Pt electrocatalyst CoN_x/C has been prepared by Zhang et al. [238] via a chelation process using cobaltous nitrate and imidazole as cobalt and nitrogen precursors respectively. As it can be seen from Fig. 15, this cathode electrocatalyst exhibited relatively good performance (200 mW cm^{-2}; anode Pt loading: 300 $\mu g\,cm^{-2}$). Recently, for the first time in the literature, Ma et al. [239] prepared an ORR Co-N_4 electrocatalyst through pyrolysis of carbon-supported cobalt triethylenetetramine chelate under an argon atmosphere. They used a new, cheap and simple ligand, triethylenetetramine (TETA), which has four nitrogen atoms, as nitrogen-containing precursor to substitute porphyrins and pthalocyanines. The performance of a H_2-PEMFC with CoTETA/C as cathode and Pt as anode with a Pt loading of 400 $\mu g\,cm^{-2}$ reached 135 mW cm^{-2} at room temperature (Fig. 15), showing its potential application as non-Pt ORR catalyst. Jaouen et al. [240] used cyanamide as nitrogen precursor and black pearls 2000 as support, which exhibited very good performance with 239 mW cm^{-2} at a Pt loading of 500 $\mu g\,cm^{-2}$ (compared to the results shown in Fig. 15). On the other hand, it has been proved to be not very stable.

A different highly ordered Fe-N-C catalyst has been prepared by Lei et al. [241], with greatly improved performance of 252 mW cm^{-2} (Fig. 15), compared to 60 mW cm^{-2} achieved by the amorphous Fe-N-C.

3.2.1.3. Nitrogen-modified carbon based electrocatalysts. According to Maldonado and Stevenson [242], the strong basicity of N-doped carbons facilitates the reductive O_2 adsorption and the decomposition of peroxide species, thereby increasing the ORR catalytic activity. Among the examined catalysts shown in Fig. 15, Co-Fe-N chelate complex, investigated by Popov et al. [243], exhibited the highest power density of 529 mW cm^{-2} under H_2-PEMFC working conditions. In this cell, carbon supported Pt (500 $\mu g_{Pt}\,cm^{-2}$) was used as anode catalyst. The above Co-Fe-N/C electrocatalyst was developed through the high-temperature pyrolysis of Co-Fe-N chelate complex on the support followed by chemical leaching. Moreover, as the authors reported [243], for 480 h fuel cell continuous operation no significant performance decrease has been observed. Several groups have developed such kind of catalysts [244–247], among them Yeager et al. [247] also showed that Co/N/C catalyst was capable of reducing oxygen in an acidic medium. Dodelet et al. [248] investigated Fe/N/C catalyst using ammonia to add N-bearing functionalities. From Fig. 15, it can also be distiguished that its electrocatalytic activity is not poor as the maximum power density of fuel cell reaches 234 mW cm^{-2} with anode Pt loading of 300 $\mu g\,cm^{-2}$. Additionally, very recently Kim et al. [246] prepared novel nitrogen modified carbon nanofibers by pyrolysis of cobalt. This electrocatalyst under fuel cell operation exhibited a good performance of 335 mW cm^{-2} (anode Pt loading: 400 $\mu g_{Pt}\,cm^{-2}$, Fig. 15) and significantly improved stability. Subramanian et al. [249] also prepared nitrogen-modified carbon-based catalyst by oxidizing carbon black with nitric acid followed by chemical modification with nitrogen-rich precursors such as melamine, urea, thiourea and selenourea. Its application as cathode electrocatalyst in a H_2-PEMFC led to a maximum power density of 188 mW cm^{-2} (anode Pt loading: 500 $\mu g\,cm^{-2}$, Fig. 15).

Also N-doped ordered porous carbon catalysts with polyacrylonitrile as both carbon and nitrogen precursor [250] possessed high catalytic activity toward ORR with a maximum power density of 306 mW cm^{-2} (Fig. 15). In the case that polyaniline was used as both carbon and nitrogen precursor, the cell maximum power density reached the value of 380 mW cm^{-2} (1.52 mW $\mu g_{Pt_{total}}^{-1}$) [251]. In both cases, the anode's Pt loading was relatively low; 500 $\mu g\,cm^{-2}$

and 250 $\mu g\,cm^{-2}$ respectively. Polyacrylonitrile was also used by Mastragostino et al. [252] in combination with iron citrate to prepare mesoporous xerogel carbon as non-Pt catalyst for ORR. However, their catalytic activity compared to the other electrocatalysts, shown in Fig. 15, was very poor with a power density of 10 $mW\,cm^{-2}$ (anode Pt loading: 500 $\mu g\,cm^{-2}$).

Among the most recent reported nitrogen-modified carbon catalysts, the best performance under fuel cell operating conditions has been obtained over a catalyst prepared from aromatic polyamides, poly(meta-phenylene isopthalamide) (MPIA) mixed with $FeCl_2$ by pyrolysis [253]. The fuel cell maximum power density reached 480 $mW\,cm^{-2}$, while the Pt loading at the anode compartment was 500 $\mu g\,cm^{-2}$. According to Zelenay et al. [254], cyanamide is a really good nitrogen precursor. Using cynamide as cathode and Pt (250 $\mu g\,cm^{-2}$) as anode, the H_2-PEMFC exhibited a maximum power density of 370 $mW\,cm^{-2}$. Nagai et al. [255] also tried to combine the properties of nitrogen-doped carbon supports with tungsten and they obtained in a H_2-PEMFC performance of 382 $mW\,cm^{-2}$ (anode Pt loading: 400 $\mu g\,cm^{-2}$).

3.2.1.4. Transition metal carbides, nitrides and oxynitrides. In a general overview, transition metals (binary and ternary alloys of them) carbides, nitrides and oxynitrides [256] exhibited performances remarkably equal to or better than that of commercial Pt catalysts with the same loading. For example, as it can be seen from Fig. 15, when the binary alloy of palladium-titanium was used as cathode in a H_2-PEMFC, the measured maximum power density value was ca. 190 $mW\,cm^{-2}$ ($\sim$1 $mW\,\mu g^{-1}_{Pt_{total}}$), with anode Pt loading to be 200 $\mu g\,cm^{-2}$ (Fig. 15). Transition metal carbides and nitrides are two major kinds of electrode materials recently investigated, due to their good electrical conductivity, corrosion resistance and electrocatalytic activity [141]. The advantage of combining WC with a transition metal seems to derive mainly from WC, which itself is able to enhance the catalytic activity, apart from its synergistic effect with the transition metal. Since Boudart and Levy [257] reported the Pt-like properties of tungsten carbide (WC) for H_2-O_2 titration, carbides and nitrides have been intensively investigated for their suitability to substitute Pt in PEMFCs [258].

Comparable to tungsten carbides, tungsten nitrides have not been intensively investigated as electrocatalysts for PEMFCs. However, their unique electrochemical properties and stability in electrolytes within a wide pH range make them promising electrocatalysts for PEMFCs. Recently, in an effort to improve the electrocatalytic activity and stability, tungsten and molybdenum nitrides were also investigated in a single fuel cell under sulphuric acidic environment [259,260]. However, compared to the rest ORR catalysts, summarized in Fig. 15, their electrocatalytic activity was not very high (39.2 $mW\,cm^{-2}$ [259] and 65 $mW\,cm^{-2}$ [260]).

Concerning the oxynitrides, they exhibited almost the same behaviour as carbides and nitrides [261,262]. It has been established that factors such as the high heat-treatment temperature affect the crystalline structure and increase the chemical stability and activity.

Metal carbonitrides is another class of potential non-Pt electrocatalysts for ORR. However, compared to carbides and nitrides, carbonitrides seem to be less popular. Recently, these compounds have also attracted some attention due to their electrochemical properties and stability [263,264].

3.2.1.5. Transition metal chalcogenides. Since 1986, when Alonso-Vante and Tributsch [265] reported Ru-Mo-Se chalcogenides as ORR catalysts, the last two decades transition metal chalcogenides have been studied as one of the most promising materials among the non-noble transition metal catalysts for ORR [266]. In Fig. 15 is reported $RuFeN_x/C$ [266] as cathode electrocatalyst in a H_2-PEMFC, which exhibited 180 $mW\,cm^{-2}$ (400 $\mu g_{Pt}\,cm^{-2}$ of anode Pt loading). Based on the structure, these materials could be classified into two types: (i) the Chevrel phase-type compounds such as $Mo_4Ru_2Se_8$, and (ii) the amorphous phase compounds such as Ru_xSe_y [267]. The promoting role of Se in the activity of Ru_xSe_y in acid environment was examined by Savinova et al. [268]. According to the authors, Se hindered the dissociative adsorption of oxygen on Ru due to the electronic interaction with the latter, suggesting that the adsorption of electronegative atoms, such as S, O, Cl on the surface of noble and transition metals lead to a notable increase of the metal's work function. Moreover, Bron et al. [269] examined the influence of Se on the catalytic properties of Ru-based catalysts for ORR in acid electrolytes. The dependence of ORR activity on Se/Ru ratio exhibited a volcano-type behaviour with about a 10 fold increase of the mass activity at $0.1 < Se/Ru < 0.3$. Lately, Solorza-Feria et al. [270] reported a comparative study and electrochemical evaluation of $Ru_xM_ySe_z$ (M = Cr, Mo, W) electrocatalysts towards ORR, according to RDE measurements. In all cases, a 4-electron reduction mechanism has been proposed. The catalytic activity towards ORR decreased according to the following order: $Ru_xMo_ySe_z > Ru_xW_ySe_z > Ru_xCr_ySe_z$. However, this trend was not respected when the materials were tested as cathode electrodes in a single PEMFC. The $Ru_xW_ySe_z$ electrocatalyst exhibited poor activity compared with $Ru_xMo_ySe_z$ and $Ru_xCr_ySe_z$, which were considered as suitable candidates to be used as cathodes in PEMFCs. The major drawback of these kinds of ORR catalysts is their instability under fuel cell operation conditions. However, recently Zhang et al. [271] employed titanium dioxide for modifying the carbon black supporting material of the $Ru_{85}Se_{15}$ catalyst. The examined electrocatalyst, not only presented good performance (171 $mW\,cm^{-2}$, Fig. 15), but also provided a favourable influence on the electrochemical stability to a certain extent during the H_2-PEMFC's operation (anode Pt loading: 400 $\mu g\,cm^{-2}$) operation. A good candidate for ORR catalyst is also the tellurioum chalcogenide, which in this case was used to modify the carbon support [272]. The maximum power density obtained in this case was 270 $mW\,cm^{-2}$, while the Pt loading was 500 $\mu g_{Pt}\,cm^{-2}$ (Fig. 15).

3.2.1.6. Iridium-based electrocatalysts. Among the Pt-group metals, iridium is one of the most stable in acidic media and for this reason lately has attracted much interest. Qiao et al. [273] investigated nanostructured Ir-V/C electrocatalyst for the ORR in a H_2-PEMFC. The iridium modified with vanadium showed improved catalytic activity and selectivity following the four electron reduction of O_2 to H_2O. A maximum power density of 517 $mW\,cm^{-2}$ (Fig. 15) was obtained where the cell presented a stable performance for $\sim$100 h. The Pt loading at the anode compartment was 400 $\mu g_{Pt}\,cm^{-2}$. This is the second best H_2-PEMFC performance obtained according to the results shown in Fig. 15. On the other hand, Nagao et al. [150] examined iridium oxide, for the ORR in a H_2-PEMFC, which exhibited only 20 $mW\,cm^{-2}$ (anode Pt loading: 1000 $\mu g\,cm^{-2}$).

3.2.1.7. Palladium-based electrocatalysts. Due to their high catalytic activity and their excellent chemical stability, Pd-based electrocatalysts are widely used for the ORR in PEMFCs. The most common examined binary and ternary alloys are Pd-M (M = Co [274,275], Ti [256,276], Cu [277,278], Ni [279]) or Pd-Co-M (M = Au [256,276], Mo [264,276], Ce [274], Ni [280]) and others [278,281]. From Fig. 15, it can be recognized that the fourth best studied ORR catalyst is $Pd_{80}Ni_{20}/C$ [279] with 400 $mW\,cm^{-2}$ of maximum power density, with an anode Pt loading of 400 $\mu g\,cm^{-2}$. This electrocatalyst was prepared according to a modified polyol method, followed by heat treatment at 500 °C. Good performance was obtained on a ternary Pd-Co-Ni based supported on carbon nitride heat-treated electrocatalyst (Pd-Co-Ni/CN) [280]. Using it as cathode

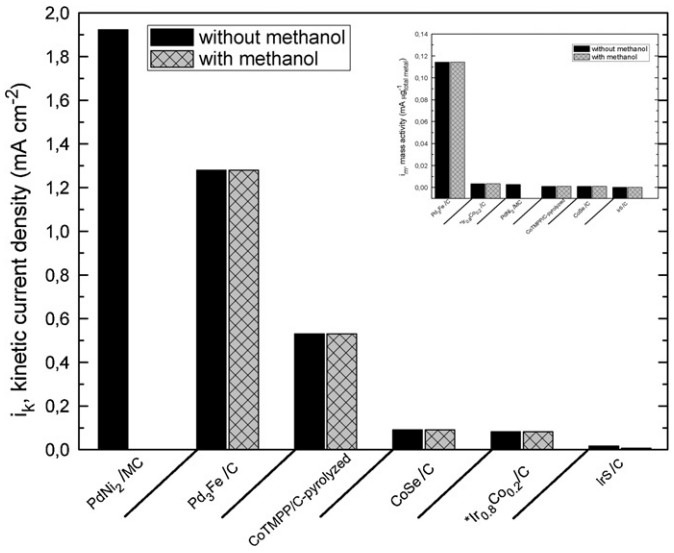

Fig. 16. Kinetic currents (mA cm^{-2}) (at 0.8 V, 1600 rpm) for *Oxygen Reduction Reaction* over non-platinum electrocatalysts in presence and in absence of methanol [*400 rpm, **the catalyst did not examine with the RDE technique in presence of methanol]. Inset: mass activities in terms of (mA $\mu g^{-1}_{metal\ loading}$).

and Pt (1000 $\mu g\,cm^{-2}$) as anode catalyst respectively, the maximum power density of the fuel cell reached 256 mW cm^{-2} (Fig. 15). However taking into consideration the high Pt loading is required, the cost problem still remains.

3.2.2. Direct methanol fuel cells – DMFCs

It is clearly reported that, in the development of advanced cathode catalysts for DMFCs, the parasitic reaction that takes place on the cathode and is caused by both sluggish ORR and methanol crossover, should be diminished as much as possible. Therefore Pt-free cathode catalysts with high performance and tolerance to methanol are required. In the case of DMFCs the most examined non-Pt catalysts can be classified as follows: (i) Porphyrin-based macrocyclic compounds of transition metal, (ii) Transition Metal Carbides and Nitrides, and (iii) Transition Metal Chalcogenides.

3.2.2.1. Porphyrin-based macrocyclic compounds of transition metal. The porphyrins-based macrocyclic compounds of transition metals can also be considered as a potential electrocatalysts for ORR in a DMFC. However, according to the literature [282], the performance of these catalysts in acidic media is not stable and it is significantly improved by pyrolyzing them. In Fig. 16 CoTMPP (tetra-methoxy-phenyl-porphyrin)/C-pyrolyzed electrocatalyst [283] presented kinetic current density 0.53 mA cm^{-2} vs. RHE (530 $\mu g_{metal\ loading}$ cm^{-2}) towards ORR and very high methanol tolerance according to RDE measurements. In presence of methanol, the kinetic current remained at the value of 0.53 mA cm^{-2}. Moreover, Atanassov and Zelenay et al. [284] measured high ORR selectivity and high fuel cell performance (142 mW cm^{-2}), using pyrolyzed CoTMPP as cathode and Pt-Ru/C as anode (4 mg_{Pt} cm^{-2}). It was proposed that in the temperature range of 500–700 °C these catalysts presented a N_4 – metal structure, bounded with the carbon support. The catalytic activity of pyrolyzed non-precious ORR catalysts was greatly dependent on the heat-treatment conditions. Based on the above discussion, it is generally accepted that heat treatment has a beneficial effect on both activity and stability of these electrocatalysts. However, the cost of this class of non-Pt catalysts is high, because macrocycles are expensive materials.

3.2.2.2. Transition metal chalcogenides. Although there have not been intensive efforts to study transition metal chalcogenides for DMFCs, new challenges in this area have been recently reported. Ruthenium based compounds containing selenium (Ru_xSe_y) have been investigated [285–287] as alternative low cost non-Pt catalysts. In particular, non-precious transition metal chalcogenides have attracted considerable attention because of their: (i) high fuel tolerance, (ii) promising catalytic activity, (iii) high stability, although they still have relatively lower catalytic activities for ORR than Pt-based catalysts [288].

The good methanol tolerance of chalcogenide-based electrocatalysts is shown in Fig. 16. Cobalt-selenium carbon supported ORR catalyst [289] exhibited a relatively low activity, 0.091 mA cm^{-2} vs SHE (91 $\mu g_{metal\ loading}$ cm^{-2}), which remained the same even in presence of methanol. Palladium-selenium catalyst [290] has also shown a good activity and an excellent tolerance towards ORR.

Chalcogenide-based catalysts were also examined under DMFCs operation conditions [285,291,292]. Very recently, Jeng et al. [292] synthesized and studied a ruthenium selenide (RuSe) supported on carbon nanotubes (CNTs) electrocatalyst. They reported [292] that the performance of DMFC (45 mW cm^{-2}) using RuSe/CNT as cathode was higher than that having Pt/C cathode and strongly dependent on the carbon support. Thus, some promising results of ruthenium (Ru)-based chalcogenides and a series of Ru_xX_y chalcogenide, (X = S, Se and Te) showed in acidic media high ORR activity and high methanol tolerance. However, among the transition metals – including Pt – that have been used for the M-chalcogenides, Ir is one of the most stable metals in acidic media. Recently, a novel methanol-tolerant ORR catalyst, iridium-selenium (Ir-Se) chalcogenide has been studied by Zhang et al. [293] and exhibited relatively high catalytic activity. In this case, it was found that most of oxygen could be directly reduced to water through the 4-electron pathway, with less than 10% of hydrogen peroxide (H_2O_2) production. This enhancement compared to that of pure Ir might be attributed to the bimetallic interaction effect. Zhang et al. [294] also investigated Ir_xCo_{1-x} alloy for ORR. Compared to Pt/C catalysts, IrCo alloys have much stronger methanol tolerance in terms of ORR onset potential and performance. As it can be distiguished from Fig. 16, IrCo/C has presented relatively low kinetic current, 0.082 mA cm^{-2} vs RHE, (25 $\mu g_{metal\ loading}$ cm^{-2}), but strong methanol tolerance. It was also confirmed that this catalyst can catalyze the complete four-electron transfer reaction, converting oxygen to water. Recently, a novel methanol-tolerant reduction catalyst, IrS/C is proposed by Ma et al. [133]. However, its catalytic activity is not very high compared with the rest of the catalysts reported in Fig. 16.

Further improvements of the transition metal chalcogenides, e.g., via elemental modification and compositional modulation are required to substantially increase the catalytic activity of ORR, conserving at the same time high methanol tolerance.

3.2.2.3. Palladium-based and other non platinum-transition metals. In the previous years, three research groups [295–297] identified a family of very promising ORR cobalt–palladium alloy electrocatalysts. A significant amount of works was necessary to completely characterize these materials, clarifying the role of composition in the catalytic activity, testing performance stability and mechanism elucidation. The results of this effort are also depicted in Fig. 16. As it can be seen according to the CV's results the highest activity, 1.92 mA cm^{-2} vs NHE (711 μg_{Pd} cm^{-2}), has been achieved by the bimetallic palladium-nickel electrocatalyst supported on mesoporous carbon [298], remaining stable in the presence of methanol. Moreover, the bi-metallic catalyst palladium-iron [299] presented the second best activity, 1.28 mA cm^{-2} vs. RHE (~11 μg_{Pd} cm^{-2}). In presence of methanol the PdFe/C cathode catalyst's activity remained constant. Prakash et al. [275] examined the catalytic

activity of carbon supported $CoPd_x$ (x = 1, 2, 3, 4, 5 and 9) for ORR in a single PEMFC. The ORR mechanism was evaluated on $CoPd_3$ and it was found that the rate-determining step was a chemical step that followed a fast first electron transfer and this may involve the breaking of the oxygen bond on the $CoPd_3$ surface. The $CoPd_3$ catalyst showed good chemical stability during PEMFC operation and – compared to Pt – enhanced tolerance to the crossovered methanol.

Non Pt-catalysts such as palladium-based catalysts have shown promising catalytic activities and methanol tolerance properties. Lately, the above-mentioned class of Ir-based catalysts appeared as one of the most stable catalysts in acidic media.

3.2.2.4. Nitrogen-based precursors and nitrogen-modified carbon based electrocatalysts. Currently, very few research works have been devoted to nitrogen-based precursors for preparing cathode electrocatalysts for DMFCs. Recently Liu et al. [295] reported a carbon-containing iron nitride electro-catalyst by chelating N-containing species and Fe^{2+} with a carbon support, under heat treatment in an NH_3 atmosphere, which presented very good ORR activity. Moreover, Fe-N_x/C with 2,3,5,6-tetra(2-pyridyl)pyrazine (TPPZ) to be employed as ligand to prepare an iron complex (Fe-TPPZ) that served as a precursor [296], was tested as cathode in a DMFC. The TPPZ is a nitrogen containing precursor which plays a critical role in achieving ORR activity as well as stability during the M-N_x synthesis. The fuel cell performance reached the value of 160 mW cm^{-2}. The anode's Pt loading was 300 μg cm^{-2}. Wei et al. [297] considered melamine as a rich source of nitrogen and they used it for the preparation of iron or cobalt based nitrogen-doped carbon aerogels. These aerogels were used as cathode in a DMFC, exhibiting relatively low power density, despite the fact that the anode Pt loading was very high (4 mg cm^{-2}).

3.2.3. Direct ethanol fuel cells – DEFCs

As far as DEFCs are concerned, one of the major challenges -as in the case of DMFCs- is the poor performance of their Pt-free cathode catalysts. However, Pt-free catalysts such as porphyrin-based macrocyclic compounds of transition metal, carbides, nitrides, oxynitrides and transition metal chalcogenides have not been still examined in DEFCs.

3.2.3.1. Other transition metals. According to the literature results depicted in Fig. 17 the highest activity 1.8 mA cm^{-2} vs. RHE (51 $\mu g_{metal\ loading}$ cm^{-2}) is observed over Ru/C electrocatalyst [300]. As it can be seen, in presence of ethanol the kinetic current remains the same. On the other hand, the performance of a DEFC based on a 20% Ru/C cathode (5 mW cm^{-2}; anode Pt loading: 1 mg cm^{-2}) was lower than that observed over 20% Pt/C cathode (17 mW cm^{-2}). According to Viswanathan et al. [301] among the various bimetallic Pd-based alloy Pd-Co with a third metal exhibited good activity values and close to that of Pt/C. The second best activity, 1.6 mA cm^{-2} vs. NHE was obtained over Pd-Co-Mo/Carbon black-heat treated at 973 K [301]. Its catalytic activity was reduced only by *ca.* 7% in the presence of ethanol. The Pd-Co-Mo was also successfully examined as cathode in a DEFC. The power density was 8 mW cm^{-2} with 1 mW cm^{-2} of Pt loading as anode catalyst and remained stable for 50 h. The Pd-Co [302] exhibited the same activity, 1.5 mA cm^{-2} vs RHE, with Pd-Co-Mo/Carbon black-heat treated electrocatalyst, which reduced by 0.7 mA cm^{-2} in presence of ethanol.

Concerning the Co-Se [289] and Pd_3Fe [303] cathode electrocatalysts, their catalytic activity is not as high as that of the rest catalysts shown in Fig. 17, but it is higher than that of Pt/C and their ethanol tolerance is excellent. The Co-Se bimetallic catalyst belongs to the class of transition chalcogenides as part of the effort to develop novel Pt-free electrocatalysts. The oxygen reduction reaction on PdFe has been studied by Adzic et al. [304] and its kinetics and mechanism have been reported by Zhutaeva et al. [305]. Then Song et al. [303] assured that the optimum ratio palladium: iron was 3:1.

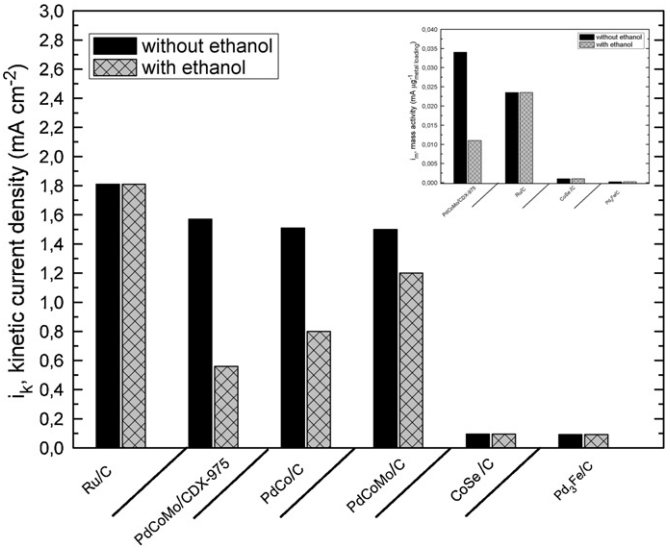

Fig. 17. Kinetic currents (mA cm^{-2}) (at 0.8 V, 1600 rpm) for *Oxygen Reduction Reaction* over non-platinum electro-catalysts in presence and in absence of ethanol. Inset: mass activities in terms of (mA $\mu g^{-1}_{metal\ loading}$).

Finally, by comparing Figs. 17 and 10 it is obvious that, concerning their electrocatalytic activity and ethanol tolerance, non-Pt ORR cathodes are superior to low Pt ones.

Non-Pt electrocatalysts have also been examined under DEFCs operation conditions. More precisely, a DEFC, which was less prone to ethanol crossover, with Ni-Co-Fe (NCF) as cathode catalyst has been reported by Park et al. [306]. The decrease of the open circuit voltage of DEFC with NCF electrocatalysts was less than that with Pt/C as cathode catalysts at high ethanol concentrations. The NCF electrocatalyst was less prone to ethanol oxidation at the cathode even when ethanol crossover occurred through Nafion-117® membrane, which avoided the voltage drop at the cathode. However, Pt loading (PtRu/C) at anode compartment was very high and consequently it is not attractive for applications. Moreover, a Co-PPY(polypyrrole)-MWCNTs composite for ORR has been developed by Ramaprabhu et al. [233]. The peak performance of the DEFC using commercially Co/MWCNT as cathode and PtRu/MWCNT as anode was 23 mW cm^{-2}, while using Co-PPY-MWCNTs (home-made) as cathode and Pt-Sn/MWCNT as anode (Pt loading: 2.5 mg cm^{-2}) reached 33 mW cm^{-2}. Here, the increase of the fuel cell performance has been attributed to the higher electronic conductivity of the MWCNTs than that of the carbon black, as well as to the uniform dispersion of catalytic particles over the large surface of MWCNTs.

4. Conclusions

The target of 5 mW $\mu g^{-1}_{Pt_{total}}$ that has been set by the United States Department of Energy has been exceeded as far as the H_2-PEMFCs are concerned. The best maximum mass specific power density (MSPD) under H_2-PEMFC operating conditions reached 260 mW $\mu g^{-1}_{Pt_{total}}$, over a binary Pt-Pd/C (1 μg_{Pt} cm^{-2}) anode and low Pd/C cathode, while the highest power density, 1200 mW cm^{-2}, has been obtained in a H_2-PEMFC with an ultra-low Pt anode electrocatalyst (100 μg cm^{-2}) prepared by a modified thin film method and a low Pt/C (100 μg cm^{-2}) as cathode.

The highest maximum mass specific power density under DMFC operating conditions reached ~0.15 mW $\mu g^{-1}_{Pt_{total}}$ over

PtRu/Vulcan-XC-72 (Pt loading: 250 $\mu g\,cm^{-2}$) anode and Pt/MWCMTs (Pt loading: 250 $\mu g\,cm^{-2}$) cathode, while the highest power density, 210 $mW\,cm^{-2}$ (MSPD: 0.09 $mW\,\mu g^{-1}_{Pt_{total}}$), has been obtained in a DMFC with a PtRu supported on mesoporous carbon as anode (Pt loading: 1300 $\mu g\,cm^{-2}$) and Pt/C (1000 $\mu g\,cm^{-2}$) as cathode.

The highest maximum mass specific power density under DEFC operating conditions reached ~0.05 $mW\,\mu g^{-1}_{Pt_{total}}$ over a ternary PtRuIrSn (Pt loading: 287 $\mu g\,cm^{-2}$) anode and the same cathode (Pt loading: 287 $\mu g\,cm^{-2}$), while the highest power density, 105 $mW\,cm^{-2}$ (MSPD: ~0.047 $mW\,\mu g^{-1}_{Pt_{total}}$), has been obtained in a DEFC with a PtRu/C (Pt loading: 1246 $\mu g\,cm^{-2}$) as anode and Pt/C (1000 $\mu g\,cm^{-2}$) as cathode.

Concerning the non-Pt electrocatalysts the highest maximum mass specific power density under H_2-PEMFC operating conditions reached ~1.5 $mW\,\mu g^{-1}_{Pt_{total}}$ over PANI (polyaniline)-FeCo/C cathode and Pt-catalyzed cloth GDL (E-Tek), (Pt loading: 250 $\mu g\,cm^{-2}$) anode, while the highest maximum power density, 1000 $mW\,cm^{-2}$, in a H_2-PEMFC was obtained by a carbon supported 40%Ir–10%V/C anode and Pt/C (300 $\mu g_{Pt}\,cm^{-2}$) cathode.

Moreover, among the non-Pt electrocatalysts the highest electrocatalytic activity towards MOR, ~20 $mA\,cm^{-2}$, under CV's measurements, has been displayed by $Pd/TiO_{2nanotubes}$, while for EOR, ~13 $mA\,cm^{-2}$, by the binary IrSn/C alloy. The IrSn/C also performed semi-equal performance in a DEFC with Pt/C electrocatalyst as concerns both activity and stability. The maximum power density in this case was 38 $mW\,cm^{-2}$. Finally, PdNi/MC (mesoporous carbon) and Ru/C showed the highest kinetic current density, ~1.9 $mA\,cm^{-2}$ and ~1.8 $mA\,cm^{-2}$, respectively, towards ORR in absence and in presence of methanol and ethanol, in RDE's measurements.

Acknowledgements

A. Brouzgou, is grateful to the Research Funding Program: Heracleitus II which is co-financed by the European Union (European Social Fund – ESF) and Greek national funds through the Operational Program "Education and Lifelong Learning" of the National Strategic Reference Framework (NSRF) -Investing in knowledge society through the European Social Fund. *S.Q. Song*, is grateful to the Project of NSFC (20903122, 21276290) and the Fundamental Research Funds for the Central Universities (Guangzhou) (09lgpy30), and the grant from Hi-Tech Research and Development Program of China (2009AA05Z110). Finally, the present research was also partially supported by the "SYNERGASIA" Program (09SYN-32-615: ECHOCO2) which is co-financed by the European Union and the Greek Ministry of Development-GSRT.

References

[1] H.A. Gasteiger, S.S. Kocha, B. Sompalli, F.T. Wagner, Applied Catalysis B-Environmental 56 (1–2) (2005) 9–35.
[2] X. Yu, S. Ye, Journal of Power Sources 172 (1) (2007) 133–144.
[3] *Platinum Today* Available from: [http://www.platinum.matthey.com/pgm-prices/price-charts/].
[4] S. Vengatesan, H.-J. Kim, S.-K. Kim, I.-H. Oh, S.-Y. Lee, E. Cho, H.Y. Ha, T.-H. Lim, Electrochimica Acta 54 (2) (2008) 856–861.
[5] H.A. Gasteiger, S.S. Kocha, B. Somaplli, F.T. Wagner, Applied Catalysis B-Environmental 56 (2005) 9–35.
[6] F. Alcaide, G. Álvarez, P.L. Cabot, O. Miguel, A. Querejeta, International Journal of Hydrogen Energy 35 (20) (2010) 11634–11641.
[7] M. Götz, H. Wendt, Electrochimica Acta 43 (24) (1998) 3637–3644.
[8] C. He, H.R. Kunz, J.M. Fenton, Journal of the Electrochemical Society 150 (8) (2003) A1017–A1024.
[9] G.L. Holleck, D. Pasquariello, S. Clauson, in: S. Gottesfeld (Ed.), The Electrochemical Society Proceedings Series Pennignton: Proton Conducting Membrane Fuel Cells, T.F. Fuller, Pennington, 1999.
[10] R. Venkataraman, H.R. Kunz, J.M. Fenton, Journal of the Electrochemical Society 150 (2003) A278–A284.
[11] T. Yamanaka, T. Takeguchi, G. Wang, E.N. Muhamad, W. Ueda, Journal of Power Sources 195 (19) (2010) 6398–6404.
[12] P.P. Lopes, E.A. Ticianelli, H. Varela, Journal of Power Sources 196 (1) (2011) 84–89.
[13] J.H. Kim, B. Fang, M. Kim, J.-S. Yu, Catalysis Today 146 (1–2) (2009) 25–30.
[14] E. Yoo, T. Okada, T. Akita, M. Kohyama, I. Honma, J. Nakamura, Journal of Power Sources 196 (1) (2011) 110–115.
[15] Y. Wang, K.S. Chen, J. Mishler, S.C. Cho, X.C. Adroher, Applied Energy 88 (4) (2011) 981–1007.
[16] Y.-H. Cho, B. Choi, Y.-H. Cho, H.-S. Park, Y.-E. Sung, Electrochemistry Communications 9 (3) (2007) 378–381.
[17] E. Antolini, S.C. Zignani, S.F. Santos, E.R. Gonzalez, Electrochimica Acta 56 (5) (2011) 2299–2305.
[18] L. Xiong, A. Manthiram, Electrochimica Acta 50 (16–17) (2005) 3200–3204.
[19] M. Cavarroc, A. Ennadjaoui, M. Mougenot, P. Brault, R. Escalier, Y. Tessier, J. Durand, S. Roualdès, T. Sauvage, C. Coutanceau, Electrochemistry Communications 11 (2009) 859–861.
[20] D. Gruber, N. Ponath, J. Mγóller, F. Lindstaedt, Journal of Power Sources 150 (2005) 67–72.
[21] R. Zeis, A. Mathur, G. Fritz, J. Lee, J. Erlebacher, Journal of Power Sources 165 (1) (2007) 65–72.
[22] M. Carmo, V.A. Paganin, J.M. Rosolen, E.R. Gonzalez, Journal of Power Sources 142 (1–2) (2005) 169–176.
[23] T. Ioroi, N. Fujiwara, Z. Siroma, K. Yasuda, Y. Miyazaki, Electrochemistry Communications 4 (5) (2002) 442–446.
[24] R. O'hayre, S.-J. Lee, S.-W. Cha, F.B. Prinz, Journal of Power Sources 109 (2) (2002) 483–493.
[25] A.D. Taylor, M. Michel, R.C. Sekol, J.M. Kizuka, N.A. Kotov, L.T. Thompson, Advanced Functional Materials 18 (19) (2008) 3003–3009.
[26] C.-H. Wan, Q.-H. Zhuang, International Journal of Hydrogen Energy 32 (17) (2007) 4402–4411.
[27] T. Ioroi, Z. Siroma, N. Fujiwara, S.-I. Yamazaki, K. Yasuda, Electrochemistry Communications 7 (2) (2005) 183–188.
[28] W.-C. Chang, M.T. Nguyen, Journal of Power Sources 196 (14) (2011) 5811–5816.
[29] C.-H. Wan, M.-T. Lin, Q.-H. Zhuang, C.-H. Lin, Surface and Coating Technology 201 (1–2) (2006) 214–222.
[30] N. Cunningham, E. Irissou, M. Lefevre, M.C. Denis, D. Guay, J.P. Dodelet, Electrochemical and Solid State Letters 6 (7) (2003) A125–A128.
[31] S.S. Pethaiah, G.P. Kalaignan, G. Sasikumar, M. Ulaganathan, Solid State Ionics 190 (1) (2011) 88–92.
[32] S. Chen, Z. Wei, H. Li, L. Li, Chemical Communications 46 (46) (2010) 8782–8784.
[33] A.C. Garcia, V.A. Paganin, E.A. Ticianelli, Electrochimica Acta 53 (12) (2008) 4309–4315.
[34] D.C. Papageorgopoulos, M. Keijzer, J.B.J. Veldhuis, F.A. De Bruijn, Journal of the Electrochemical Society 149 (11) (2002) A1400–A1404.
[35] R.A. Antunes, M.C.L. De Oliveira, G. Ett, V. Ett, Journal of Power Sources 196 (6) (2011) 2945–2961.
[36] H. Liu, C. Song, L. Zhang, J. Zhang, H. Wang, D.P. Wilkinson, Journal of Power Sources 155 (2) (2006) 95–110.
[37] S.H. Ahn, O.J. Kwon, S.-K. Kim, I. Choi, J.J. Kim, International Journal of Hydrogen Energy 35 (24) (2010) 13309–13316.
[38] J.-S. Choi, W.S. Chung, H.Y. Ha, T.-H. Lim, I.-H. Oh, S.-A. Hong, H.-I. Lee, Journal of Power Sources 156 (2) (2006) 466–471.
[39] J.F. Whitacre, T. Valdez, S.R. Narayanan, Journal of the Electrochemical Society 152 (9) (2005) A1780–A1789.
[40] Y. Ando, K. Sasaki, R. Adzic, Electrochemistry Communications 11 (6) (2009) 1135–1138.
[41] E.A. Franceschini, G.A. Planes, F.J. Williams, G.J.A.A. Soler-Illia, H.R. Corti, Journal of Power Sources 196 (4) (2011) 1723–1729.
[42] P. Justin, G. Ranga Rao, International Journal of Hydrogen Energy 36 (10) (2011) 5875–5884.
[43] X. Wang, J. Zhang, H. Zhu, Chinese Journal of Catalysis 32 (1) (2011) 74–79.
[44] N. Kakati, J. Maiti, S.H. Jee, S.H. Lee, Y.S. Yoon, Journal of Alloy Compound 509 (18) (2011) 5617–5622.
[45] J. Cao, C. Du, S.C. Wang, P. Mercier, X. Zhang, H. Yang, D.L. Akins, Electrochemistry Communications 9 (4) (2007) 735–740.
[46] Y. Chen, G. Zhang, J. Ma, Y. Zhou, Y. Tang, T. Lu, International Journal of Hydrogen Energy 35 (19) (2010) 10109–10117.
[47] I.-S. Park, E. Lee, A. Manthiram, Journal of the Electrochemical Society 157 (2) (2010) B251–B255.
[48] G. Girishkumar, K. Vinodgopal, P.V. Kamat, Journal of Physical Chemistry B 108 (52) (2004) 19960–19966.
[49] J.J. Wang, G.P. Yin, J. Zhang, Z.B. Wang, Y.Z. Gao, Electrochimica Acta 52 (24) (2007) 7042–7050.
[50] Q.-Z. Jiang, X. Wu, M. Shen, Z.-F. Ma, X.-Y. Zhu, Catalysis Letters 124 (3) (2008) 434–438.
[51] M. Khosravi, M.K. Amini, International Journal of Hydrogen Energy 35 (19) (2010) 10527–10538.
[52] D. Wang, Y. Liu, J. Huang, T. You, Journal of Colloid and Interface Science 367 (1) (2011) 199–203.
[53] G. Wu, Y.-S. Chen, B.-Q. Xu, Electrochemistry Communications 7 (12) (2005) 1237–1243.
[54] Y. Xin, J.-G. Liu, Y. Zhou, W. Liu, J. Gao, Y. Xie, Y. Yin, Z. Zou, Journal of Power Sources 196 (3) (2011) 1012–1018.

[55] G. Cui, P.K. Shen, H. Meng, J. Zhao, G. Wu, Journal of Power Sources 196 (15) (2011) 6125–6130.
[56] S.M. Choi, M.H. Seo, H.J. Kim, W.B. Kim, Carbon 49 (3) (2011) 904–909.
[57] C.-T. Hsieh, W.-M. Hung, W.-Y. Chen, J.-Y. Lin, International Journal of Hydrogen Energy 36 (4) (2011) 2765–2772.
[58] H. Zhao, L. Li, J. Yang, Y. Zhang, H. Li, Electrochemistry Communications 10 (6) (2008) 876–879.
[59] Z. Cui, L. Feng, C. Liu, W. Xing, Journal of Power Sources 196 (5) (2011) 2621–2626.
[60] H.J. Wang, H. Yu, F. Peng, P. Lv, Electrochemistry Communications 8 (3) (2006) 499–504.
[61] V. Neburchilov, H. Wang, J. Zhang, Electrochemistry Communications 9 (7) (2007) 1788–1792.
[62] G. Wu, B.-Q. Xu, Journal of Power Sources 174 (1) (2007) 148–158.
[63] Y.-N. Wu, S.-J. Liao, Z.-X. Liang, L.-J. Yang, R.-F. Wang, Journal of Power Sources 194 (2) (2009) 805–810.
[64] S. Liao, K.-A. Holmes, H. Tsaprailis, V.I. Birss, Journal of American Chemical Society 128 (11) (2006) 3504–3505.
[65] R. Wang, H. Li, H. Feng, H. Wang, Z. Lei, Journal of Power Sources 195 (4) (2010) 1099–1102.
[66] J. Yang, X. Chen, F. Ye, C. Wang, Y. Zheng, J. Yang, Journal of Materials Chemistry 21 (25) (2011) 9088–9094.
[67] C.W. Mason, A.M. Kannan, ISRN Nanotechnology 2011 (2011) 6.
[68] S. Tang, G. Sun, J. Qi, S. Sun, J. Guo, Q. Xin, G.M. Haarberg, Chinese Journal of Catalysis 31 (1) (2010) 12–17.
[69] Y. Wang, C. He, A. Brouzgou, Y. Liang, R. Fu, D. Wu, P. Tsiakaras, S. Song, Journal of Power Sources 200 (2012) 8–13.
[70] F. Colmati, E. Antolini, E.R. Gonzalez, Electrochimica Acta 50 (28) (2005) 5496–5503.
[71] J. Qi, L. Jiang, Q. Tang, S. Zhu, S. Wang, B. Yi, G. Sun, Carbon 50 (8) (2012) 2824–2831.
[72] A.S. Aricò, V. Baglio, E. Modica, A. Di Blasi, V. Antonucci, Electrochemistry Communications 6 (2) (2004) 164–169.
[73] X. Xue, J. Ge, C. Liu, W. Xing, T. Lu, Electrochemistry Communications 8 (8) (2006) 1280–1286.
[74] E. Yoo, T. Okada, T. Kizuka, J. Nakamura, Journal of Power Sources 180 (1) (2008) 221–226.
[75] A. Caillard, C. Coutanceau, P. Brault, J. Mathias, J.M. Léger, Journal of Power Sources 162 (1) (2006) 66–73.
[76] M. Carmo, M. Brandalise, A.O. Neto, E.V. Spinacé, A.D. Taylor, M. Linardi, J.O.G. Rocha Poço, International Journal of Hydrogen Energy 36 (22) (2011) 14659–14667.
[77] A. Murthy, E. Lee, A. Manthiram, Applied Catalysis B-Environmental 121–122 (2012) 154–161.
[78] H. Du, B. Li, F. Kang, R. Fu, Y. Zeng, Carbon 45 (2) (2007) 429–435.
[79] E. You, R. Guzmán-Blas, E. Nicolau, M. Aulice Scibioh, C.F. Karanikas, J.J. Watkins, C.R. Cabrera, Electrochimica Acta 75 (2012) 191–200.
[80] G. Wang, G. Sun, Q. Wang, S. Wang, H. Sun, Q. Xin, International Journal of Hydrogen Energy 35 (20) (2010) 11245–11253.
[81] X. Xue, T. Lu, C. Liu, W. Xu, Y. Su, Y. Lv, W. Xing, Electrochimica Acta 50 (16–17) (2005) 3470–3478.
[82] Z. Cui, C. Liu, J. Liao, W. Xing, Electrochimica Acta 53 (27) (2008) 7807–7811.
[83] A.S. Aricò, P. Creti, P.L. Antonucci, V. Antonucci, Electrochemical and Solid State Letters 1 (2) (1998) 66–68.
[84] Y. Wang, S. Song, G. Andreadis, H. Liu, P. Tsiakaras, Journal of Power Sources 196 (11) (2011) 4980–4986.
[85] H. Wang, Z. Jusys, R.J. Behm, Journal of Power Sources 154 (2) (2006) 351–359.
[86] E. Antolini, Journal of Power Sources 170 (1) (2007) 1–12.
[87] J. Liu, J. Ye, C. Xu, S.P. Jiang, Y. Tong, Electrochemistry Communications 9 (9) (2007) 2334–2339.
[88] A. Kowal, M. Li, M. Shao, K. Sasaki, M.B. Vukmirovic, J. Zhang, N.S. Marinkovic, P. Liu, A.I. Frenkel, R.R. Adzic, Nature Materials 8 (4) (2009) 325–330.
[89] J. Datta, S.S. Gupta, S. Singh, S. Mukherjee, M. Mukherjee, Materials and Manufacturing Processes 26 (2) (2011) 261–271.
[90] H. Li, D. Kang, H. Wang, R. Wang, International Journal of Electrochemical Science 6 (2011) 1058–1065.
[91] X. Yang, J. Zheng, M. Zhen, X. Meng, F. Jiang, T. Wang, C. Shu, L. Jiang, C. Wang, Applied Catalysis B-Environmental 121–122 (2012) 57–64.
[92] W. Du, D. Su, Q. Wang, A.I. Frenkel, X. Teng, Crystal Growth and Design 11 (2) (2011) 594–599.
[93] J.M. Sieben, M.M.E. Duarte, International Journal of Hydrogen Energy 36 (5) (2011) 3313–3321.
[94] J. Ma, H. Sun, F. Su, Y. Chen, Y. Tang, T. Lu, J. Zheng, International Journal of Hydrogen Energy 36 (12) (2011) 7265–7274.
[95] H. Zhang, C. Hu, X. He, L. Hong, G. Du, Y. Zhang, Journal of Power Sources 196 (10) (2011) 4499–4505.
[96] L. Yu, J. Xi, Electrochimica Acta 67 (2012) 166–171.
[97] L. Frolova, N. Lyskov, Y. Dobrovolsky, Solid State Ionics (2012), http://dx.doi.org/10.1016/j.ssi.2012.02.013, in press.
[98] S. Song, C. He, J. Liu, Y. Wang, A. Brouzgou, P. Tsiakaras, Applied Catalysis B-Environmental 119–120 (2012) 227–233.
[99] B. Liu, Z.-W. Chia, Z.-Y. Lee, C.-H. Cheng, J.-Y. Lee, Z.-L. Liu, Journal of Power Sources 206 (0) (2012) 97–102.
[100] P. Xiao, X. Guo, D.-J. Guo, H.-Q. Song, J. Sun, Z. Lv, Y. Liu, X.-P. Qiu, W.-T. Zhu, L.-Q. Chen, U. Stimming, Electrochimica Acta 58 (2011) 541–550.
[101] Q. Wang, G.Q. Sun, L. Cao, L.H. Jiang, G.X. Wang, S.L. Wang, S.H. Yang, Q. Xin, Journal of Power Sources 177 (1) (2008) 142–147.
[102] Z. Mingyuan, S. Gongquan, L. Huanqiao, C. Lei, X. Qin, Chinese Journal of Catalysis 29 (8) (2008) 765–770.
[103] H. Li, G. Sun, L. Cao, L. Jiang, Q. Xin, Electrochimica Acta 52 (24) (2007) 6622–6629.
[104] L. Jiang, G. Sun, S. Sun, J. Liu, S. Tang, H. Li, B. Zhou, Q. Xin, Electrochimica Acta 50 (27) (2005) 5384–5389.
[105] P.E. Tsiakaras, Journal of Power Sources 171 (1) (2007) 107–112.
[106] X. Xue, J. Ge, T. Tian, C. Liu, W. Xing, T. Lu, Journal of Power Sources 172 (2) (2007) 560–569.
[107] R.F.B. De Souza, L.S. Parreira, D.C. Rascio, J.C.M. Silva, E. Teixeira-Neto, M.L. Calegaro, E.V. Spinacé, A.O. Neto, M.C. Santos, Journal of Power Sources 195 (6) (2010) 1589–1593.
[108] A.O. Neto, L.A. Farias, R.R. Dias, M. Brandalise, M. Linardi, E.V. Spinacé, Electrochemistry Communications 10 (9) (2008) 1315–1317.
[109] D.F. Silva, A.N. Geraldes, A.O. Neto, E.S. Pino, M. Linardi, E.V. Spinacé, W.A.A. Macedo, J.D. Ardisson, Materials Science and Engneering 175 (3) (2010) 261–265.
[110] R.F.B. De Souza, L.S. Parreira, J.C.M. Silva, F.C. Simões, M.L. Calegaro, M.J. Giz, G.A. Camara, A.O. Neto, M.C. Santos, International Journal of Hydrogen Energy 36 (18) (2011) 11519–11527.
[111] M. Zhu, G. Sun, Q. Xin, Electrochimica Acta 54 (5) (2009) 1511–1518.
[112] J. Tayal, B. Rawat, S. Basu, International Journal of Hydrogen Energy 36 (22) (2011) 14884–14897.
[113] E. Lee, A. Murthy, A. Manthiram, Electrochimica Acta 56 (3) (2011) 1611–1618.
[114] K. Fatih, V. Neburchilov, V. Alzate, R. Neagu, H. Wang, Journal of Power Sources 195 (21) (2010) 7168–7175.
[115] J. Perez, V.A. Paganin, E. Antolini, Journal of the Electroanalytical Chemistry 654 (1–2) (2011) 108–115.
[116] J. Ribeiro, D.M. Dos Anjos, K.B. Kokoh, C. Coutanceau, J.M. Léger, P. Olivi, A.R. De Andrade, G. Tremiliosi-Filho, Electrochimica Acta 52 (24) (2007) 6997–7006.
[117] T.S. Almeida, L.M. Palma, P.H. Leonello, C. Morais, K.B. Kokoh, A.R. De Andrade, Journal of Power Sources 215 (2012) 53–62.
[118] S.C. Zignani, V. Baglio, J.J. Linares, G. Monforte, E.R. Gonzalez, A.S. Aricò, Electrochimica Acta 70 (2012) 255–265.
[119] E. Ribadeneira, B.A. Hoyos, Journal of Power Sources 180 (1) (2008) 238–242.
[120] D.R. Lycke, E.D.L. Gyenge, Electrochimica Acta 52 (13) (2007) 4287–4298.
[121] J. Tayal, B. Rawat, S. Basu, International Journal of Hydrogen Energy 37 (5) (2012) 4597–4605.
[122] F.C. Simões, D.M. Dos Anjos, F. Vigier, J.M. Léger, F. Hahn, C. Coutanceau, E.R. Gonzalez, G. Tremiliosi-Filho, A.R. De Andrade, P. Olivi, K.B. Kokoh, Journal of Power Sources 167 (1) (2007) 1–10.
[123] J. Prabhuram, T.S. Zhao, Z.K. Tang, R. Chen, Z.X. Liang, Journal of Physical Chemistry B 110 (11) (2006) 5245–5252.
[124] M.Y. Wang, J.H. Chen, Z. Fan, H. Tang, G.H. Deng, D.L. He, Y.F. Kuang, Carbon 42 (2004) 3251–3272.
[125] R.V. Parthasarathy, V.P. Menon, C.R. Martin, Chemistry of Materials 9 (2) (1997) 560–566.
[126] A.A. Gewirth, M.S. Thorum, Inorganic Chemistry 49 (8) (2010) 3557–3566.
[127] A. Morozan, B. Jousselme, S. Palacin, Energy and Environmental Science 4 (4) (2011) 1238–1254.
[128] H. Yang, W. Vogel, C. Lamy, N.S. Alonso-Vante, Journal of Physical Chemistry B 108 (30) (2004) 11024–11034.
[129] K.-S. Lee, S.J. Yoo, D. Ahn, S.-K. Kim, S.J. Hwang, Y.-E. Sung, H.-J. Kim, E. Cho, D. Henkensmeier, T.-H. Lim, J.H. Jang, Electrochimica Acta 56 (24) (2011) 8802–8810.
[130] S. Dsoke, A. Moretti, G. Giuli, R. Marassi, International Journal of Hydrogen Energy 36 (13) (2011) 8098–8102.
[131] M. Oezaslan, P. Strasser, Journal of Power Sources 196 (12) (2011) 5240–5249.
[132] U.A. Paulus, T.J. Schmidt, H.A. Gasteiger, R.J. Behm, Journal of the Electroanalytical Chemistry 495 (2) (2001) 134–145.
[133] J. Ma, D. Ai, X. Xie, J. Guo, Particuology 9 (2) (2011) 155–160.
[134] R. Wang, X. Li, H. Li, Q. Wang, H. Wang, W. Wang, J. Kang, Y. Chang, Z. Lei, International Journal of Hydrogen Energy 36 (10) (2011) 5775–5781.
[135] Q. Huang, H. Yang, Y. Tang, T. Lu, D.L. Akins, Electrochemistry Communications 8 (8) (2006) 1220–1224.
[136] S.M.S. Kumar, N. Hidyatai, J.S. Herrero, S. Irusta, K. Scott, International Journal of Hydrogen Energy 36 (9) (2011) 5453–5465.
[137] S. Zhang, Y. Shao, G. Yin, Y. Lin, Applied Catalysis B-Environmental 102 (3–4) (2011) 372–377.
[138] J. Ma, Y. Tang, G. Yang, Y. Chen, Q. Zhou, T. Lu, J. Zheng, Applied Surface Science 257 (15) (2011) 6494–6497.
[139] M.K. Jeon, Y. Zhang, P.J. Mcginn, Electrochimica Acta 55 (19) (2010) 5318–5325.
[140] D. Van Der Vliet, C. Wang, M. Debe, R. Atanasoski, N.M. Markovic, V.R. Stamenkovic, Electrochimica Acta 56 (24) (2011) 8695–8699.
[141] Y. Wang, S. Song, V. Maragou, P.K. Shen, P. Tsiakaras, Applied Catalysis B-Environmental 89 (1–2) (2009) 223–228.
[142] C. He, S. Song, J. Liu, V. Maragou, P. Tsiakaras, Journal of Power Sources 195 (21) (2010) 7409–7414.
[143] M.J. Liao, Z.D. Wei, S.G. Chen, L. Li, M.B. Ji, Y.Q. Wang, International Journal of Hydrogen Energy 35 (15) (2010) 8071–8079.
[144] W. Li, Z. Chen, L. Xu, Y. Yan, Journal of Power Sources 195 (9) (2010) 2534–2540.

[145] S. Mukerjee, S. Srinivasan, Journal of the Electroanalytical Chemistry 357 (1–2) (1993) 201–224.
[146] U.A. Paulus, A. Wokaun, G.G. Scherer, T.J. Schmidt, V. Stamenkovic, V. Radmilovic, N.M. Markovic, P.N. Ross, Journal of Physical Chemistry B 106 (16) (2002) 4181–4191.
[147] V. Di Noto, E. Negro, Journal of Power Sources 195 (2) (2010) 638–648.
[148] B. Fic ilar, A. Bayrakc eken, İ. Eroğlu, Journal of Power Sources 193 (1) (2009) 17–23.
[149] S. Thanasilp, M. Hunsom, Renewable Energy 36 (6) (2011) 1795–1801.
[150] C.H. Chang, T.S. Yuen, Y. Nagao, H. Yugami, Journal of Power Sources 195 (18) (2010) 5938–5941.
[151] W.-P. Zhou, K. Sasaki, D. Su, Y. Zhu, J.X. Wang, R.R. Adzic, Journal of Physical Chemistry C 114 (19) (2010) 8950–8957.
[152] L. Dubau, F. Maillard, M. Chatenet, J. André, E. Rossinot, Electrochimica Acta 56 (2) (2010) 776–783.
[153] L. Dubau, J. Durst, F. Maillard, L. Guétaz, M. Chatenet, J. André, E. Rossinot, Electrochimica Acta 56 (28) (2011) 10658–10667.
[154] M. Mougenot, A. Caillard, P. Brault, S. Baranton, C. Coutanceau, International Journal of Hydrogen Energy 36 (14) (2011) 8429–8434.
[155] N. Ramaswamy, T.M. Arruda, W. Wen, N. Hakim, M. Saha, A. Gullá, S. Mukerjee, Electrochimica Acta 54 (26) (2009) 6756–6766.
[156] N. Rajalakshmi, H. Ryu, M.M. Shaijumon, S. Ramaprabhu, Journal of Power Sources 140 (2) (2005) 250–257.
[157] X. Li, S. Park, B.N. Popov, Journal of Power Sources 195 (2) (2010) 445–452.
[158] K.S. Lyons, P.J. Bouwman, N.P. Ugarte, Low-Platinum Catalysts for Oxygen Reduction at Proton Exchange Membrane Fuel Cell Cathodes, in Hydrogen, Fuel Cells and Infrastructure Technology, F.Y.P. report, Editor, 2003.
[159] P. Mani, R. Srivastava, P. Strasser, Journal of Power Sources 196 (2) (2011) 666–673.
[160] W. Trongchuankij, K. Poochinda, K. Pruksathorn, M. Hunsom, Renewable Energy 35 (12) (2010) 2839–2843.
[161] S. Takenaka, A. Hirata, E. Tanabe, H. Matsune, M. Kishida, Journal of Catalysis 274 (2) (2010) 228–238.
[162] K.L. Huang, C.H. Tsai, Y.C. Lai, W.J. Lee, 209th ECS Meeting (2006).
[163] L. Xiong, A.M. Kannan, A. Manthiram, Electrochemistry Communications 4 (11) (2002) 898–903.
[164] J.W. Kim, B. Lim, H.-S. Jang, S.J. Hwang, S.J. Yoo, J.S. Ha, E.A. Cho, T.-H. Lim, S.W. Nam, S.-K. Kim, International Journal of Hydrogen Energy 36 (1) (2011) 706–712.
[165] S.-Y. Huang, P. Ganesan, B.N. Popov, Applied Catalysis B-Environmental 96 (1–2) (2010) 224–231.
[166] T. Kottakkat, A.K. Sahu, S.D. Bhat, P. Sethuraman, S. Parthasarathi, Applied Catalysis B-Environmental 110 (2011) 178–185.
[167] P. Hernández-Fernández, M. Montiel, P. Ocón, J.L.G. De La Fuente, S. García-Rodríguez, S. Rojas, J.L.G. Fierro, Applied Catalysis B-Environmental 99 (1–2) (2010) 343–352.
[168] F. Alcaide, G. Álvarez, O. Miguel, M.J. Lázaro, R. Moliner, A. López-Cudero, J. Solla-Gullón, E. Herrero, A. Aldaz, Electrochemistry Communications 11 (5) (2009) 1081–1084.
[169] R.I. Jafri, N. Rajalakshmi, S. Ramaprabhu, Journal of Power Sources 195 (24) (2010) 8080–8083.
[170] M.S. Saha, A.F. Gullá, R.J. Allen, S. Mukerjee, Electrochimica Acta 51 (22) (2006) 4680–4692.
[171] J. Zhao, K. Jarvis, P. Ferreira, A. Manthiram, Journal of Power Sources 196 (10) (2011) 4515–4523.
[172] M. Shao, B. Merzougui, K. Shoemaker, L. Stolar, L. Protsailo, Z.J. Mellinger, I.J. Hsu, J.G. Chen, Journal of Power Sources 196 (18) (2011) 7426–7434.
[173] H. Perez, A. Morin, L. Akrour, C. Cremona, B. Baret, J. Haccoun, S. Escribano, A. Etcheberry, Electrochimica Acta 55 (7) (2010) 2358–2362.
[174] Z.D. Wei, Y.C. Feng, L. Li, M.J. Liao, Y. Fu, C.X. Sun, Z.G. Shao, P.K. Shen, Journal of Power Sources 180 (1) (2008) 84–91.
[175] J.M. Tang, K. Jensen, M. Waje, W. Li, P. Larsen, K. Pauley, Z. Chen, P. Ramesh, M.E. Itkis, Y. Yan, R.C. Haddon, Journal of Physical Chemistry C 111 (48) (2007) 17901–17904.
[176] C.V. Rao, A.L.M. Reddy, Y. Ishikawa, P.M. Ajayan, Carbon 49 (3) (2011) 931–936.
[177] B. Fang, J. Luo, P.N. Njoki, R. Loukrakpam, D. Mott, B. Wanjala, X. Hu, C.-J. Zhong, Electrochemistry Communications 11 (6) (2009) 1139–1141.
[178] S. Woo, I. Kim, J.K. Lee, S. Bong, J. Lee, H. Kim, Electrochimica Acta 56 (8) (2011) 3036–3041.
[179] E. Antolini, T. Lopes, E.R. Gonzalez, Journal of Alloy Compound 461 (1–2) (2008) 253–262.
[180] F. Wen, U. Simon, Chemistry of Materials 19 (14) (2007) 3370–3372.
[181] H. Yang, N. Alonso-Vante, J.-M. Léger, C. Lamy, Journal of Physical Chemistry B 108 (6) (2004) 1938–1947.
[182] L. Colmenares, E. Guerrini, Z. Jusys, K. Nagabhushana, E. Dinjus, S. Behrens, W. Habicht, H. Bönnemann, R. Behm, Journal of Applied Electrochemistry 37 (12) (2007) 1413–1427.
[183] Y. Liu, N. Zheng, W. Chao, H. Liu, Y. Wang, Electrochimica Acta 55 (20) (2010) 5617–5623.
[184] S. An, J.-H. Park, C.-H. Shin, J. Joo, E. Ramasamy, J. Hwang, J. Lee, Carbon 49 (4) (2011) 1108–1117.
[185] M.K. Jeon, J.H. Liu, K.R. Lee, J.W. Lee, P.J. Mcginn, S.I. Woo, Fuel Cells 10 (1) (2009) 93–98.
[186] S.-H. Liu, S.-C. Chen, W.-H. Sie, International Journal of Hydrogen Energy 36 (23) (2011) 15060–15067.
[187] M.K. Jeon, P.J. Mcginn, Journal of Power Sources 195 (9) (2009) 2664–2668.
[188] C. Jeyabharathi, P. Venkateshkumar, J. Mathiyarasu, K.L.N. Phani, Electrochimica Acta 54 (2) (2008) 448–454.
[189] M. Sakthivel, A. Schlange, U. Kunz, T. Turek, Journal of Power Sources 195 (20) (2010) 7083–7089.
[190] W. Li, Q. Xin, Y. Yan, International Journal of Hydrogen Energy 35 (6) (2010) 2530–2538.
[191] W. Li, C. Liang, W. Zhou, J. Qiu, G. Zhou, Q. Sun, Xin, Journal of Physical Chemistry B 107 (26) (2003) 6292–6299.
[192] J.-G. Oh, H. Kim, Journal of Power Sources 181 (1) (2008) 74–78.
[193] W. Yuan, K. Scott, H. Cheng, Journal of Power Sources 163 (1) (2006) 323–329.
[194] L. Xiong, A. Manthiram, Electrochimica Acta 49 (24) (2004) 4163–4170.
[195] J.R.C. Salgado, E. Antolini, E.R. Gonzalez, Applied Catalysis B-Environmental 57 (4) (2005) 283–290.
[196] E. Antolini, J.R.C. Salgado, L.G.R.A. Santos, G. Garcia, E.A. Ticianelli, E. Pastor, E.R. Gonzalez, Journal of Applied Electrochemistry 36 (3) (2006) 355–362.
[197] E. Antolini, J.R.C. Salgado, E.R. Gonzalez, Journal of the Electroanalytical Chemistry 580 (1) (2005) 145–154.
[198] T. Lopes, E. Antolini, E.R. Gonzalez, International Journal of Hydrogen Energy 33 (20) (2008) 5563–5570.
[199] Y. Xu, X. Lin, Journal of Power Sources 170 (1) (2007) 13–19.
[200] A. Castro Luna, A. Bonesi, W. Triaca, A. Di Blasi, A. Stassi, V. Baglio, V. Antonucci, A. Aricò, Journal of Nanoparticle Research 12 (1) (2010) 357–365.
[201] F. Simões, P. Olivi, Electrocatalysis 1 (2) (2010) 163–168.
[202] D. Morales-Acosta, D. López De La Fuente, L.G. Arriaga, G. Vargas Gutiérrez, F.J.R. Varela, International Journal of Electrochemical Science 6 (2011) 1835–1854.
[203] F.J. Rodriguez Varela, A.A. Gaona Coronado, J.C. Loyola, P.B. Qi-Zhong Jiang, Perez, Journal of New Materials for Electrochemical Systems 14 (2011) 75–80.
[204] F.J. Rodríguez Varela, O. Savadogo, Asia-Pacific Journal of Chemical Engineering 4 (1) (2009) 17–24.
[205] T. Lopes, E. Antolini, F. Colmati, E.R. Gonzalez, Journal of Power Sources 164 (1) (2007) 111–114.
[206] S.N. Pronkin, A. Bonnefont, P.S. Ruvinskiy, E.R. Savinova, Electrochimica Acta 55 (9) (2010) 3312–3323.
[207] D.J. Ham, C. Pak, G.H. Bae, S. Han, K. Kwon, S.-A. Jin, H. Chang, S.H. Choi, J.S. Lee, Chemical Communications 47 (20) (2011) 5792–5794.
[208] B. Li, J. Qiao, D. Yang, J. Zheng, J. Ma, J. Zhang, H. Wang, Electrochimica Acta 54 (24) (2009) 5614–5620.
[209] T. Xiao, H. Wang, A.P.E. York, V.C. Williams, M.L.H. Green, Journal of Catalysis 209 (2) (2002) 318–330.
[210] H. Böhm, F.A. Pohl, Wiss. Ber. AEG-Telefunken 41 (1968) 46.
[211] D. Ham, J. Lee, Energies 2 (4) (2009) 873–899.
[212] M. Nagai, M. Yoshida, H. Tominaga, Electrochimica Acta 52 (17) (2007) 5430–5436.
[213] S. Izhar, M. Yoshida, M. Nagai, Electrochimica Acta 54 (4) (2009) 1255–1262.
[214] Y. Hara, N. Minami, H. Matsumoto, H. Itagaki, Applied Catalysis A-General 332 (2) (2007) 289–296.
[215] X.G. Yang, C.Y. Wang, Applied Physics Letters 86 (22) (2005) 224104–224113.
[216] G.S. Tasic, S.S. Miljanic, M.P. Marceta Kaninski, D.P. Saponjic, V.M. Nikolic, Electrochemistry Communications 11 (11) (2009) 2097–2100.
[217] A. Anastasopoulos, J. Blake, B.E. Hayden, Journal of Physical Chemistry C 115 (39) (2011) 19226–19230.
[218] J.H. Zhang, Y.V. Gómez, A.J. Jacobson, A. Ramirez, R.R. Chianelli, 2003; Available from: http://www1.eere.energy.gov/hydrogenandfuelcells/electrocatalysts_workshop.html
[219] A. Serov, C. Kwak, Applied Catalysis B-Environmental 90 (3–4) (2009) 313–320.
[220] M.B. Zellner, J.G. Chen, Catalysis Today 99 (3–4) (2005) 299–307.
[221] T. Shobba, S.M. Mayanna, C.A.C. Sequeira, Journal of Power Sources 108 (1–2) (2002) 261–264.
[222] C.H. Lee, S.E. Bae, C.W. Lee, D.H. Jung, C.S. Kim, D.R. Shin, International Journal of Hydrogen Energy 26 (2) (2001) 175–178.
[223] M. Wang, D.-J. Guo, H.-L. Li, Journal of Solid State Electrochemistry 178 (6) (2005) 1996–2000.
[224] J.S. Rebello, P.V. Samant, J.L. Figueiredo, J.B. Fernandes, Journal of Power Sources 153 (1) (2006) 36–40.
[225] X.-M. Chen, Z.-J. Lin, T.-T. Jia, Z.-M. Cai, X.-L. Huang, Y.-Q. Jiang, X. Chen, G.-N. Chen, Analytica Chimica Acta 650 (1) (2009) 54–58.
[226] L. Cao, G. Sun, H. Li, Q. Xin, Electrochemistry Communications 9 (10) (2007) 2541–2546.
[227] C.W.B. Bezerra, L. Zhang, K. Lee, H. Liu, A.A.L.B. Marques, E.P. Marques, H. Wang, J. Zhang, Electrochimica Acta 53 (15) (2008) 4937–4951.
[228] G. Liu, X. Li, J.-W. Lee, B.N. Popov, Catalysis Science and Technology 1 (2) (2011) 207–217.
[229] J.-W. Lee, B. Popov, Journal of Solid State Chemistry 11 (10) (2007) 1355–1364.
[230] M. Lefèvre, J.P. Dodelet, P. Bertrand, Journal of Physical Chemistry B 104 (47) (2000) 11238–11247.
[231] Y. Feng, T. He, N. Alonso-Vante, Chemistry of Materials 20 (1) (2007) 26–28.
[232] Z.-F. Ma, X.-Y. Xie, X.-X. Ma, D.-Y. Zhang, Q. Ren, N. Heß-Mohr, V.M. Schmidt, Electrochemistry Communications 8 (3) (2006) 389–394.
[233] A.L. Mohana Reddy, N. Rajalakshmi, S. Ramaprabhu, Carbon 46 (1) (2008) 2–11.
[234] R. Bashyam, P. Zelenay, Nature 443 (7107) (2006) 63–66.
[235] S. Pylypenko, S. Mukherjee, T.S. Olson, P. Atanassov, Electrochimica Acta 53 (27) (2008) 7875–7883.

[236] E. Proietti, F. Jaouen, M. Lefèvre, N. Larouche, J. Tian, J. Herranz, J.-P. Dodelet, Nature Communications 2 (2011) 416.
[237] M. Lefèvre, E. Proietti, F. Jaouen, J.-P. Dodelet, Science 324 (5923) (2009) 71–74.
[238] Y. Ma, H. Zhang, H. Zhong, T. Xu, H. Jin, Y. Tang, Z. Xu, Electrochimica Acta 55 (27) 7945–7950.
[239] H.-J. Zhang, X. Yuan, L. Sun, X. Zeng, Q.-Z. Jiang, Z. Shao, Z.-F. Ma, International Journal of Hydrogen Energy 35 (7) (2011) 2900–2903.
[240] J. Tian, L. Birry, F. Jaouen, J.P. Dodelet, Electrochimica Acta 56 (9) (2011) 3276–3285.
[241] M. Lei, P.G. Li, L.H. Li, W.H. Tang, Journal of Power Sources 196 (7) (2011) 3548–3552.
[242] S. Maldonado, K.J. Stevenson, Journal of Physical Chemistry B 109 (10) (2005) 4707–4716.
[243] V. Nallathambi, J.-W. Lee, S.P. Kumaraguru, G. Wu, B.N. Popov, Journal of Power Sources 183 (1) (2008) 34–42.
[244] T. Onodera, S. Suzuki, T. Mizukami, H. Kanzaki, Journal of Power Sources 196 (19) (2011) 7994–7999.
[245] J.H. Zagal, J.P. Dodelet, F. Bedioui, 2006. N4-Macrocyclic Metal complexes, L. Springer Science+Business Media, Editor. United States of America.
[246] H.-S. Oh, J.-G. Oh, W.H. Lee, H.-J. Kim, H. Kim, International Journal of Hydrogen Energy 36 (14) (2011) 8181–8186.
[247] S. Gupta, D. Tryk, I. Bae, W. Aldred, E. Yeager, Journal of Applied Electrochemistry 19 (1) (1989) 19–27.
[248] J. Herranz, M. Lefγ¨Vre, N. Larouche, B. Stansfield, J.-P. Dodelet, Journal of Physical Chemistry C 111 (51) (2007) 19033–19042.
[249] N.P. Subramanian, X. Li, V. Nallathambi, S.P. Kumaraguru, H. Colon-Mercado, G. Wu, J.-W. Lee, B.N. Popov, Journal of Power Sources 188 (1) (2009) 38–44.
[250] G. Liu, X. Li, P. Ganesan, B.N. Popov, Applied Catalysis B-Environmental 93 (1–2) (2009) 156–165.
[251] G. Wu, Z. Chen, K. Artyushkova, F. Garzon, P. Zelenay, ECS Transactions 16 (2) (2008) 159–170.
[252] C. Arbizzani, S. Righi, F. Soavi, M. Mastragostino, International Journal of Hydrogen Energy 36 (8) (2011) 5038–5046.
[253] M. Chokai, L. Wu, Y. Nabae, S. Kuroki, T. Hayakawa, M.-A. Kakimoto, S. Miyata, Applied Catalysis A-General 401 (1–2)) (2011) 158–162.
[254] H.T. Chung, C.M. Johnston, K. Artyushkova, M. Ferrandon, D.J. Myers, P. Zelenay, Electrochemistry Communications 12 (12) (2010) 1792–1795.
[255] T. Ando, S. Izhar, H. Tominaga, M. Nagai, Electrochimica Acta 55 (8) (2010) 2614–2621.
[256] J. Fernández, V. Raghuveer, A. Manthiram, A.J. Bard, Journal of American Chemical Society 127 (38) (2005) 13100–13101.
[257] R.B. Levy, M. Boudart, Platinum-Like Behavior of Tungsten Carbide in Surface Catalysis, 1973, pp. 547–549.
[258] M. Nie, P.K. Shen, Z. Wei, Journal of Power Sources 167 (1) (2007) 69–73.
[259] H. Zhong, H. Zhang, Y. Liang, J. Zhang, M. Wang, X. Wang, Journal of Power Sources 164 (2) (2007) 572–577.
[260] H. Zhong, H. Zhang, G. Liu, Y. Liang, J. Hu, B. Yi, Electrochemistry Communications 8 (5) (2006) 707–712.
[261] Y. Shibata, A. Ishihara, S. Mitsushima, N. Kamiya, K.-I. Ota, Electrochemical and Solid State Letters 10 (2) (2007) B43–B46.
[262] A. Ishihara, S. Doi, S. Mitsushima, K.-I. Ota, Electrochimica Acta 53 (16) (2008) 5442–5450.
[263] K.-I. Ota, Y. Ohgi, K.-D. Nam, K. Matsuzawa, S. Mitsushima, A. Ishihara, Journal of Power Sources 196 (12) (2011) 5256–5263.
[264] V. Di Noto, E. Negro, Electrochimica Acta 55 (4) (2010) 1407–1418.
[265] N.A. Vante, H. Tributsch, Nature 323 (6087) (1986) 431–432.
[266] L. Liu, J.-W. Lee, B.N. Popov, Journal of Power Sources 162 (2) (2006) 1099–1103.
[267] L. Zhang, J. Zhang, D.P. Wilkinson, H. Wang, Journal of Power Sources 156 (2) (2006) 171–182.
[268] K.N. Loponov, V.V. Kriventsov, K.S. Nagabhushana, H. Boennemann, D.I. Kochubey, E.R. Savinova, Catalysis Today 147 (3–4) (2009) 260–269.
[269] M. Bron, P. Bogdanoff, S. Fiechter, I. Dorbandt, M. Hilgendorff, H. Schulenburg, H. Tributsch, Journal of the Electroanalytical Chemistry 500 (1–2) (2001) 510–517.
[270] K. Suárez-Alcántara, O. Solorza-Feria, Journal of Power Sources 192 (1) (2009) 165–169.
[271] T. Xu, H. Zhang, H. Zhong, Y. Ma, H. Jin, Y. Zhang, Journal of Power Sources 195 (24) (2010) 8075–8079.
[272] X. Li, L. Liu, J.-W. Lee, B.N. Popov, Journal of Power Sources 182 (1) (2008) 18–23.
[273] J. Qiao, R. Lin, B. Li, J. Ma, J. Liu, Electrochimica Acta 55 (28) (2010) 8490–8497.
[274] K. Kwon, K.H. Lee, S.-A. Jin, D.J. You, C. Pak, Electrochemistry Communications 13 (10) (2011) 1067–1069.
[275] W.E. Mustain, K. Kepler, J. Prakash, Electrochimica Acta 52 (5) (2007) 2102–2108.
[276] V. Raghuveer, A. Manthiram, A.J. Bard, Journal of Physical Chemistry B 109 (48) (2005) 22909–22912.
[277] D.C. Martínez-Casillas, G. Vázquez-Huerta, J.F. Pérez-Robles, O. Solorza-Feria, Journal of Power Sources 196 (10) (2011) 4468–4474.
[278] D.J. You, S.-A. Jin, K.H. Lee, C. Pak, K.H. Choi, H. Chang, Catalysis Today 185 (1) (2012) 138–142.
[279] J. Zhao, A. Sarkar, A. Manthiram, Electrochimica Acta 55 (5) (2010) 1756–1765.
[280] V. Di Noto, E. Negro, Electrochimica Acta 55 (26) (2010) 7564–7574.
[281] S. Takenaka, N. Susuki, H. Miyamoto, E. Tanabe, H. Matsune, M. Kishida, Journal of Catalysis 279 (2) (2011) 381–388.
[282] S.L. Gojkovic, S. Gupta, R.F. Savinell, Journal of the Electroanalytical Chemistry 462 (1) (1999) 63–72.
[283] C.-H. Wang, S.-T. Chang, H.-C. Hsu, H.-Y. Du, J.C.-S. Wu, L.-C. Chen, K.-H. Chen, Diamond and Related Materials 20 (3) (2011) 322–329.
[284] B. Piela, T.S. Olson, P. Atanassov, P. Zelenay, Electrochimica Acta 55 (26) (2010) 7615–7621.
[285] A.A. Serov, M. Min, G. Chai, S. Han, S. Kang, C. Kwak, Journal of Power Sources 175 (1) (2008) 175–182.
[286] G. Zehl, P. Bogdanoff, I. Dorbandt, S. Fiechter, K. Wippermann, C. Hartnig, Journal of Applied Electrochemistry 37 (12) (2007) 1475–1484.
[287] G. Liu, H. Zhang, J. Hu, Electrochemistry Communications 9 (11) (2007) 2643–2648.
[288] Y. Feng, A. Gago, L. Timperman, N. Alonso-Vante, Electrochimica Acta 56 (3) (2011) 1009–1022.
[289] P. Nekooi, M. Akbari, M.K. Amini, International Journal of Hydrogen Energy 35 (12) (2010) 6392–6398.
[290] R.N. Madhu, Singh, International Journal of Hydrogen Energy 36 (16) (2011) 10006–10012.
[291] D.C. Papageorgopoulos, F. Liu, O. Conrad, Electrochimica Acta 52 (15) (2007) 4982–4986.
[292] K.-T. Jeng, N.-Y. Hsu, C.-C. Chien, International Journal of Hydrogen Energy 36 (6) (2011) 3997–4006.
[293] K. Lee, L. Zhang, J. Zhang, Journal of Power Sources 165 (1) (2007) 108–113.
[294] K. Lee, L. Zhang, J. Zhang, Journal of Power Sources 170 (2) (2007) 291–296.
[295] C.-W. Tsai, H.M. Chen, R.-S. Liu, K. Asakura, L. Zhang, J. Zhang, M.-Y. Lo, Y.-M. Peng, Electrochimica Acta 56 (24) (2011) 8734–8738.
[296] A. Velázquez-Palenzuela, L. Zhang, L. Wang, P.L. Cabot, E. Brillas, K. Tsay, J. Zhang, Electrochimica Acta 56 (13) (2011) 4744–4752.
[297] Y. Wei, C. Shengzhou, L. Weiming, International Journal of Hydrogen Energy 37 (1) (2011) 942–945.
[298] G. Ramos-Sánchez, M.M. Bruno, Y.R.J. Thomas, H.R. Corti, O. Solorza-Feria, International Journal of Hydrogen Energy 37 (1) (2011) 31–40.
[299] M. Neergat, V. Gunasekar, R. Rahul, Journal of the Electroanalytical Chemistry 658 (1–2) (2011) 25–32.
[300] F.J. Rodriguez Varela, S.E. Gonzalez Ramirez, R.D. Klapco, Journal of New Materials for Electrochemical Systems 12 (1) (2009) 9–15.
[301] C.V. Rao, B. Viswanathan, Electrochimica Acta 55 (8) (2010) 3002–3007.
[302] O. Savadogo, F.J.R. Varela, Journal of New Materials for Electrochemical Systems 11 (2008) 69–74.
[303] S. Song, Y. Wang, P. Tsiakaras, P.K. Shen, Applied Catalysis B-Environmental 78 (3–4) (2008) 381–387.
[304] M.-H. Shao, K. Sasaki, R.R. Adzic, Journal of American Chemical Society 128 (11) (2006) 3526–3527.
[305] M.R. Tarasevich, G.V. Zhutaeva, V.A. Bogdanovskaya, M.V. Radina, M.R. Ehrenburg, A.E. Chalykh, Electrochimica Acta 52 (15) (2007) 5108–5118.
[306] N. Park, T. Shiraishi, K. Kamisugi, Y. Hara, K. Iizuka, T. Kado, S. Hayase, Journal of Applied Electrochemistry 38 (3) (2008) 371–375.